VARIATION OF SOME MECHANICAL PROPERTIES OF POLAR SNOW, CAMP CENTURY, GREENLAND

Austin Kovacs, W.F. Weeks
and
Frank Michitti

December 1969

DA TASK 1T061102B52A02

DA TASK 1T062112A13001

CORPS OF ENGINEERS, U.S. ARMY
COLD REGIONS RESEARCH AND ENGINEERING LABORATORY
HANOVER, NEW HAMPSHIRE

PREFACE

This report is the result of a joint study by Mr. Austin Kovacs and Mr. Frank Michitti, Research Civil Engineers, and Dr. W.F. Weeks, Research Glaciologist, of the U.S. Army Cold Regions Research and Engineering Laboratory. Messrs. Kovacs and Michitti are members of the Construction Engineering Branch (Mr. E.F. Lobacz, Chief), Experimental Engineering Division (Mr. K.A. Linell, Chief). Dr. Weeks is a member of the Snow and Ice Branch (Dr. C.C. Langway, Jr., Chief), Research Division (Dr. K.F. Sterrett, Chief).

The report is published under DA Task 1T062112A13001, *Cold Regions Research - Applied Research and Engineering;* and DA Task 1T061102B52A02, *Research in Earth Physics - Cold Regions and Related Environments.*

The authors wish to acknowledge the assistance of Mr. N.D. Craig during the study. Helpful suggestions regarding the general problem area were provided by Messrs. A.J. Gow, R.W. McGaw and R.O. Ramseier.

Citation of commercial products or manufacturers is for information only and does not constitute official endorsement or approval.

CONTENTS

ILLUSTRATIONS

VARIATION OF SOME MECHANICAL PROPERTIES OF POLAR SNOW, CAMP CENTURY, GREENLAND

by

Austin Kovacs, W.F. Weeks and Frank Michitti

INTRODUCTION

A recent review of studies of the unconfined compressive strength of polar snow (Kovacs, 1967) clearly shows the appreciable differences that exist between the results of different investigators. These differences are undoubtedly the result of changes in the testing procedures as well as actual differences in the snows tested. In the past the range of snow densities γ available at a given site has always been somewhat restricted: Butkovich (1958), $0.350 \leq \gamma \leq 0.640$ g/cm^3; Ramseier (1963), $0.450 \leq \gamma \leq 0.650$ g/cm^3; Smith (1965), $0.360 \leq \gamma \leq 0.720$ g/cm^3; Nakaya and Kuroiwa (1967), $0.320 \leq \gamma \leq 0.600$ g/cm^3.* Therefore, when an attempt was made to examine the variation in the strength of polar snow and ice over its complete natural density range, it was always necessary to patch together results obtained on hopefully similar samples from different locations that were measured using different test procedures and techniques.

The present study analyzes the results of a large number of measurements of the unconfined compressive strength of polar snow from Camp Century, Greenland, where it was possible to obtain samples with densities varying over essentially the complete natural density range for polar snow and ice ($0.340 \leq \gamma \leq 0.890$ g/cm^3). The loading apparatus used was designed specifically for the purpose. The variations of the static Young's modulus and the ring-tensile strength of the snow and ice were also studied.

TEST SITE

In selecting a field site for this type of study, it was desirable to choose a location where a wide density range of naturally densifying snow could be sampled. An ideal location was found in the Inclined Drift at Camp Century, Greenland. Schematic vertical and horizontal views of the drift are given in Figure 1. The drift is essentially a chain sawed excavation which starts at the bottom of a roofed trench roughly 10 m below the 1966 snow surface. Entrance to the trench is through a 70-m-long walkway from the snow surface. From the trench the drift extends 267 m at an average inclination of 20° until it reaches a depth of 100 m below the snow surface. The upper portion of the drift is roughly 3 × 3 m while the lower portion narrows to 1.6 × 2 m. A view of the lower portion of the drift is shown in Figure 2. It was, therefore, possible by coring specimens from the walls and floor of the drift to systematically vary the specimen density from 0.510 to 0.890 g/cm^3. By combining these results with the results of tests on 104 specimens obtained from a surface pit, the low end of the density range could be extended to 0.340 g/cm^3. The enclosed

*To change the units used in this paper to Système International d'Unités (S.I.) units which have recently been recommended for use in glaciology (*Journal of Glaciology*, vol. 7, no. 50, 1968, p. 151-153) the following conversions are used: 1 g/cm^3 = 1000 kg/m^3 and 1 kg/cm^2 = 0.98067 × 10^5 N/m^2.

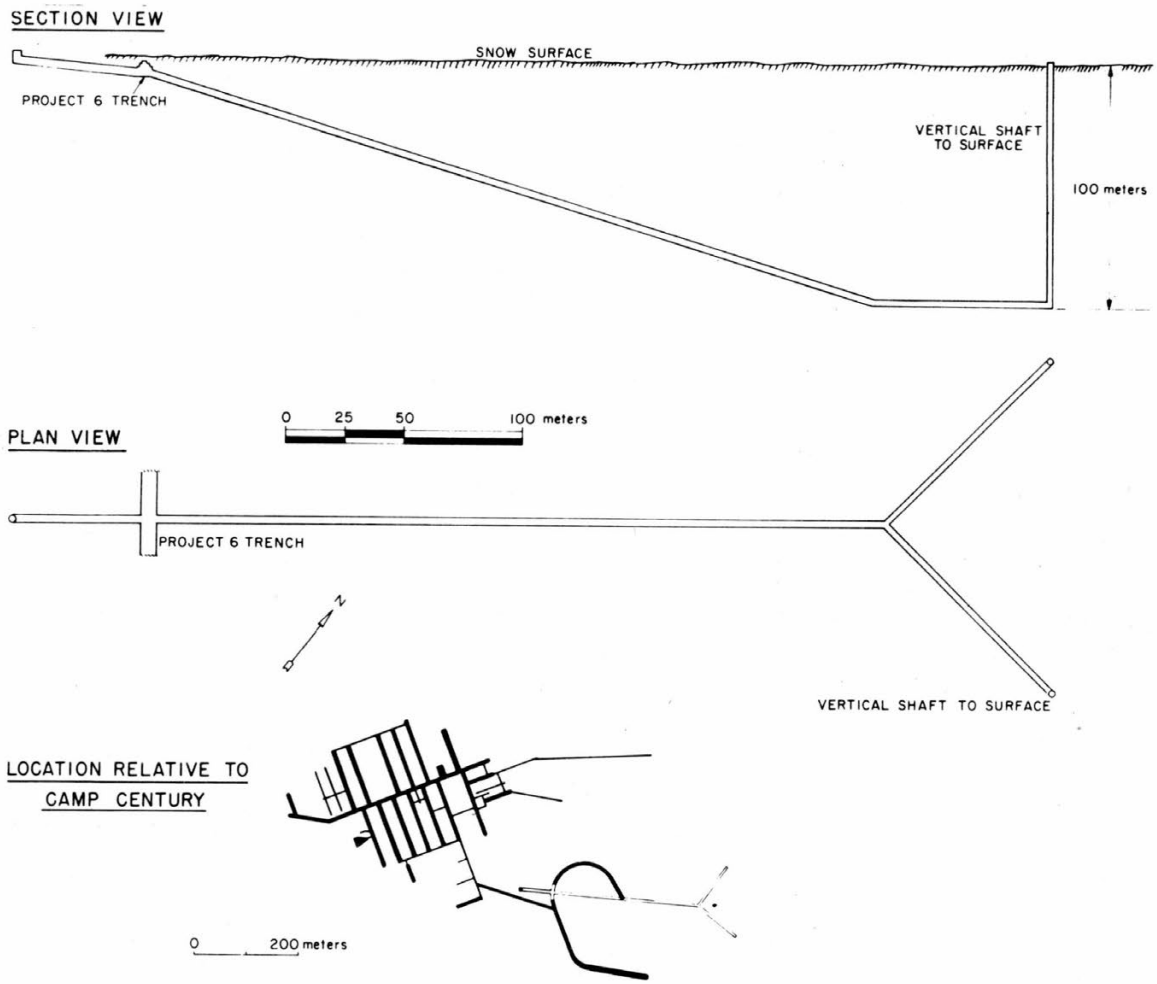

Figure 1. Schematic of the Inclined Drift, Camp Century, Greenland.

trench at the top of the drift also offered a sheltered location with a constant temperature of –25C where the specimens could be prepared and tested.

The snow in the drift had an average grain size which increased linearly with depth from 0.95 mm at 10 m to 1.95 mm at 100 m. The snow from the surface pits had an average grain size of roughly 0.5 mm. With the use of a light source behind thick-section slabs of snow, it was possible to see a stratigraphy to a depth of approximately 40 m ($\gamma \approx 0.720$ g/cm^3). Below this depth the snow was visually completely homogeneous. The snow-ice transition (γ between 0.800 and 0.830 g/cm^3) occurred at a depth of between 60 to 70 m. Pronounced ice layers indicating summer surface melt occurred at only two locations in the drift: at 9.7 m, corresponding to the warm summer of 1954 when surface melt was observed at Site 2, and at 100 m. Therefore, the snow column can, with these rare exceptions, be considered as representative of dry polar snow.

TEST PROCEDURES

Equipment

The stand of the hydraulic loading machine is of rigid construction, consisting of three 30.5- × 30.5- × 2.5-cm steel plates, four 2.5-cm-diam threaded steel rods and appropriate steel spacers

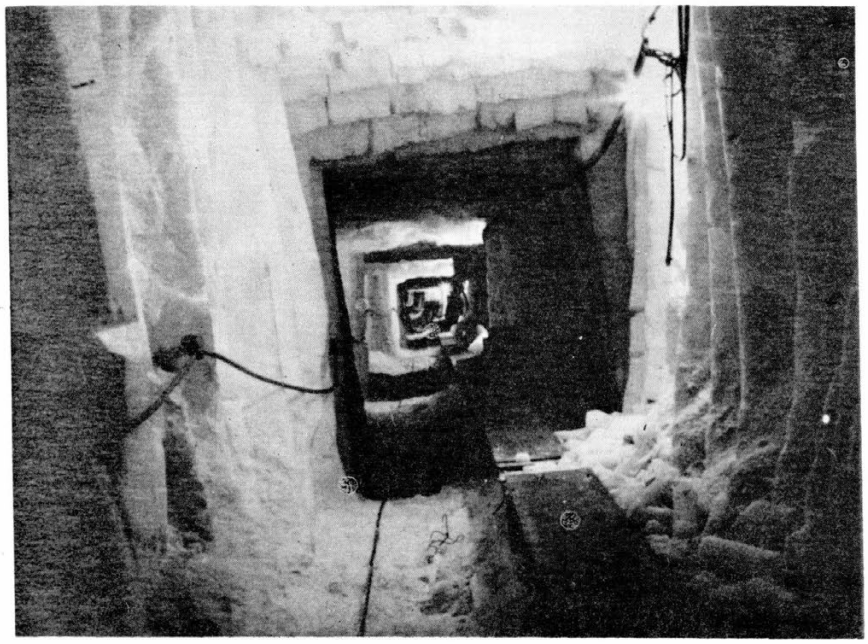

Figure 2. View of the lower portion of the drift.

as shown in Figure 3. A load cell is attached to the upper plate of the stand and a steel pivot platen is positioned beneath the load cell. The bearing surface of this platen is coated with Teflon to minimize end constraint. A hydraulic ram actuated by a high pressure hydraulic pump is located in the lower section of the loading machine. When actuated, the ram lifts the test specimen upward against the platen of the load cell from which the applied force is measured. The ram is also capped with a large Teflon-coated steel platen. Initially it was planned to regulate the ram speed. Unfortunately this was prevented by the occurrence of a fault in one of the valves during the field study.

Because this testing machine, like most, has a pivot platen, it is essential that each specimen be positioned in the test stand so that the center of the load concentration (center point of the pivot platen) is as near as possible to the geometric center of the specimen. This eliminates undesirable bending stresses associated with nonaxial loading which reduce the potential stress-carrying capacity of the specimen. The position at which test samples should be placed was determined in the field with a calibration cylinder having dimensions equivalent to those of the samples.

Three strain gauges were symmetrically located at 120° to one another on the vertical axis of the cylinder. The cylinder was then set at various locations on the ram platen until each strain gauge showed identical strains when the cylinder was loaded. The position of the outer edge of the cylinder was then inscribed on the ram platen to ensure accurate positioning of the test specimens. Even with these precautions, positioning errors and sample irregularities can give nonaxial alignments as large as 1.5 mm. Calculations (Appendix A) show that the bending stress developed by such a nonaligned load would decrease the failure strength of the specimen by 14%.

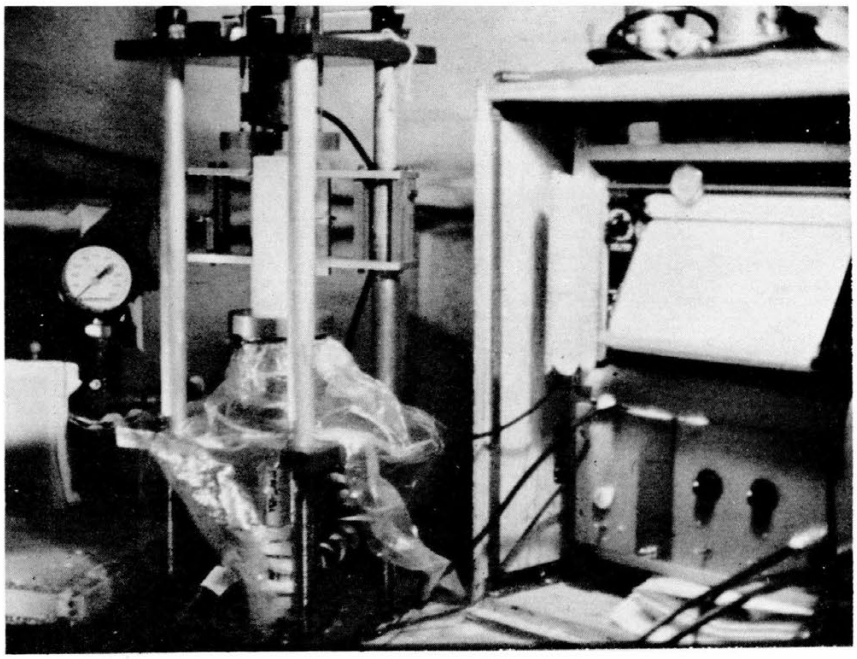

Figure 3. Testing apparatus.

A linear position transducer (LPT) was used to measure the displacement of the ram platen and the strain sustained by the specimens under load. Agreement between calibration measurements taken before and after the field study indicated that the LPT had responded properly during the tests and that the load vs strain response of the load cell had not shifted. A dual-channel, high-speed pen-type recorder was used to provide the graphic record of applied load and strain vs time during testing. The test apparatus is field portable and we believe that for its size it has an excellent capability of providing a nearly complete history of sample behavior under load up to failure.

Unconfined compression tests

A motorized Cold Regions Research and Engineering Laboratory corer was used to take smooth cylindrical cores 7.6 cm in diameter from the walls (horizontal cores) and floor (vertical cores) of the drift. The cores were cut to a fixed length and, with the use of a modified table sander, planed smooth at the ends. Extreme care was taken to ensure that the sides of the specimens were perpendicular to the ends. Final hand honing of each end face was accomplished with fine-grained emery paper to remove minor irregularities on the end faces. Such irregularities and nonparallel ends would act as stress risers which would initiate failure at bulk stress levels less than the strength of the material.

Vernier gauges were used to measure specimen length and diameter to .001 in. An average of at least three measurements was taken to establish each of these values. Final test specimens (275) were approximately 7.6 cm in diameter and 21.0 cm long for a length to diameter ratio of 2.75 to 1. This ratio was also chosen to minimize the effects of end constraint and minor end non-parallelism. A triple beam balance was used to measure specimen weight to .1 g. All measurements pertinent to each unconfined compression specimen are listed in Appendix B.

Ring tensile tests

The ring tensile strengths of 255 specimens were determined. In preparing the ring tensile specimens, the initial cores were cut into lengths of approximately 7 to 8 cm with a bandsaw. Each end was then planed smooth on the modified table sander. The length ℓ and the radius r_o of the resulting ice cylinder were determined with a vernier gauge. The specimen was positioned in a holder and a 1.27-cm coaxial hole drilled through it. The specimen was then subjected to a compressive stress by placing a diametrical load on the cylinder. The failure plane was directly beneath and parallel to the direction of the applied load. The ring tensile strength measurements are listed in Appendix C.

The theory for this test was initially developed by Ripperger and Davids (1947) and further elaborated by Assur (1958). The equation for computing the ring tensile strength σ_T is

$$\sigma_T = \frac{KP}{\pi r_o \ell}$$

where P is the load at failure and K is a stress concentration factor that depends on the external geometry of the specimen. The exact value of K is a complicated function of the ratio of the inner and outer radii r_i/r_o of the hollow cylinder. For $r_i/r_o = \frac{1}{6}$ which was used in this study the theory predicts $K = 7.09$. A detailed discussion of the results obtained from this test as applied to lake and sea ice and a general discussion of some problems relating to the test itself can be found in Weeks and Assur (1968, 1969). The test has also been applied to high density snow and glacier ice by Butkovich (1958, 1959).

TEST RESULTS

Unconfined compression

Types of failure. Figures 4-8 show typical specimen failures observed. Figure 4 shows the expulsion of grains along a failure surface. This phenomenon was often observed in the open structured snow from the surface pit that had a density of less than 0.500 g/cm^3. In this snow the weak layers were orientated horizontally and undoubtedly represented old autumn-depth hoar surfaces. It is clear in such failures that the strength record does not necessarily represent the strength of the average density of the sample but represents the structural strength of the less dense snow layer under collapse. Figure 5 shows slabbing of a sample with a density of 0.666 g/cm^3. Figures 6 and 7 show crack initiation and development prior to failure in specimens with densities between 0.850 and 0.860 g/cm^3. Note that the cracks are orientated vertically and are quite straight. For snow with a density greater than approximately 0.500 g/cm^3, failure was very rapid and often explosive in nature, as if all the strain energy within the specimen were released simultaneously (Fig. 8). This density corresponds roughly to the transition density (Anderson and Benson, 1963) where a stably bonded structure is established in thermally stable *in situ* snow. Samples having a density below 0.500 g/cm^3 also failed in a brittle manner but without the explosive nature of the higher density snows.

Failure strength vs density. The unconfined compressive strength σ_c of each specimen is listed in Appendix B and is plotted against density in Figure 9. This figure shows that the strengths of vertically and horizontally cored specimens are similar. This suggests that in the density range $\gamma > 0.600$ g/cm^3, snow behaves isotropically under unconfined compression. It is doubtful that this is still true at $\gamma < 0.500$ g/cm^3 because the horizontal planes of weakness produced by depth hoar formation have not yet been destroyed by the natural processes of compaction and recrystallization.

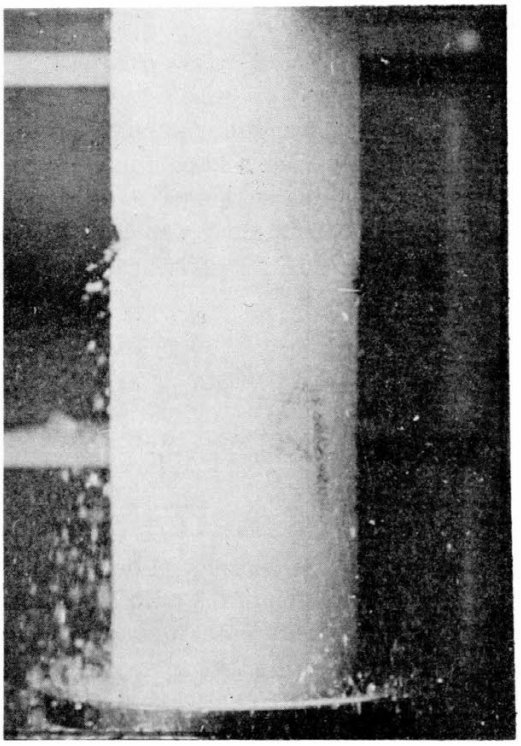

Figure 4. Failure along a horizontal depth hoar surface. Note the expulsion of grains.

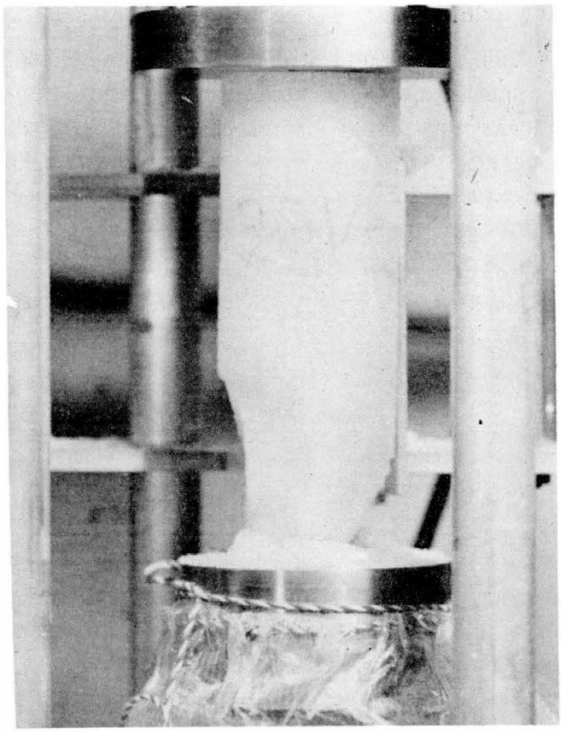

Figure 5. Slabbing of the sample.

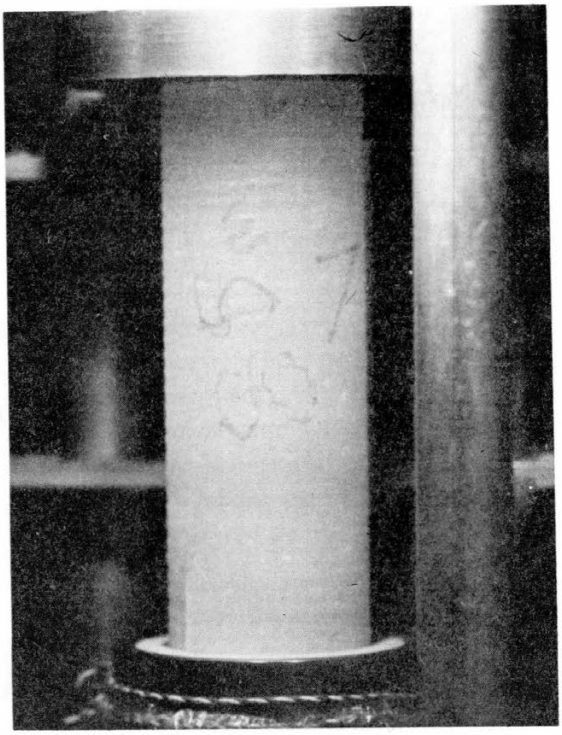

Figure 6. Crack initiation prior to failure.

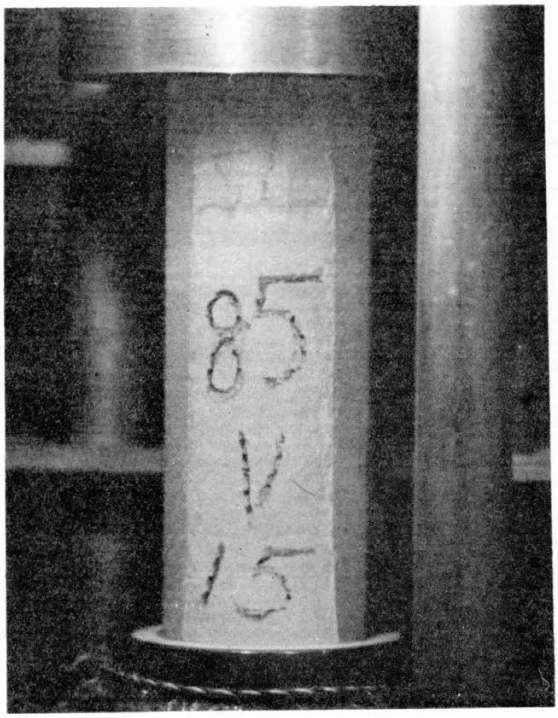

Figure 7. Crack initiation and propagation prior to failure.

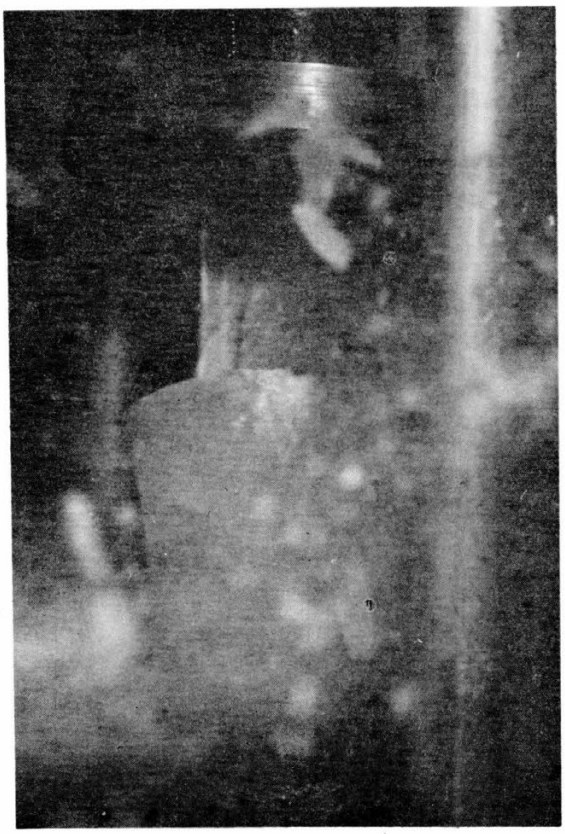

Figure 8. Explosive specimen failure.

The scatter in the unconfined compressive strength measurements does not appear to vary with density in the density range $0.340 \leq \gamma \leq 0.830$ g/cm³. At densities greater than 0.830 g/cm³, however, there is a pronounced increase in the scatter of the σ_c values. In any event the variation of σ_c with γ is clearly nonlinear. The σ_c values obtained for the vertically cored samples can be well fitted by the 4th degree polynomial

$$\sigma_c = 10^3\left(0.1462 - 1.179\gamma + 3.441\gamma^2 - 4.256\gamma^3 + 2.089\gamma^4\right) \quad (1)$$

where σ_c is expressed in kg/cm² and γ in g/cm³. Because this relation is cumbersome to use, Appendix D gives σ_c at –25C for the entire range of densities encountered at Camp Century. In addition the depth at which each density occurs is given. The depth-density curve is based on data collected by S.J. Mock* and by Langway (1967). The reader should be aware that this Appendix will not necessarily apply to other ice cap locations because of changes in the mean annual snow temperature and in the depth-density profile.

Stress and strain. The stress and strain at failure for each unconfined compression specimen are also listed in Appendix B. Groups of representative stress-strain curves for samples of different average densities are shown in Figure 10. Examination of these curves shows that in all cases there is an initial curvature prior to Hookian behavior. Careful laboratory checking showed

*Personal communication.

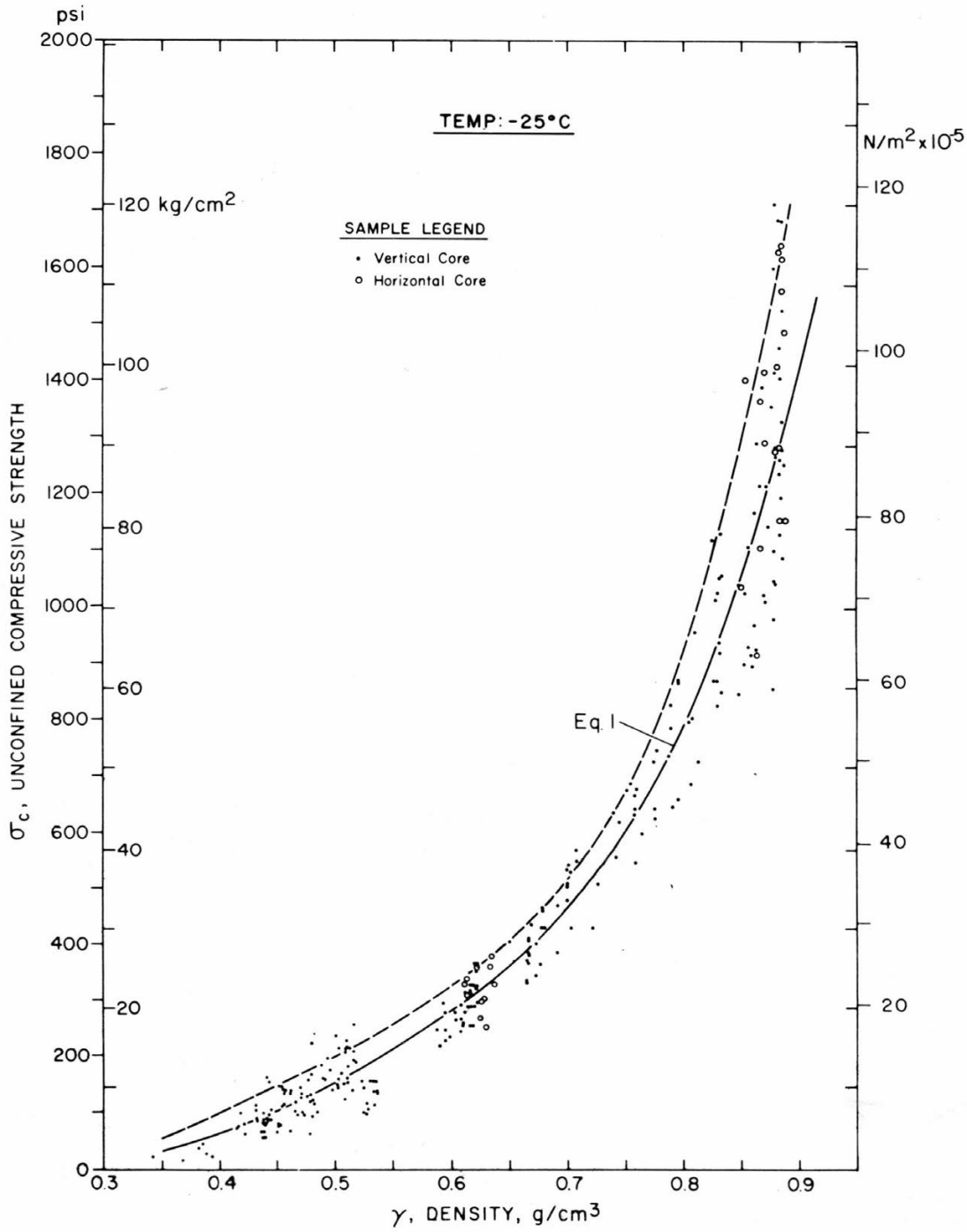

Figure 9. Unconfined compressive strength vs density.

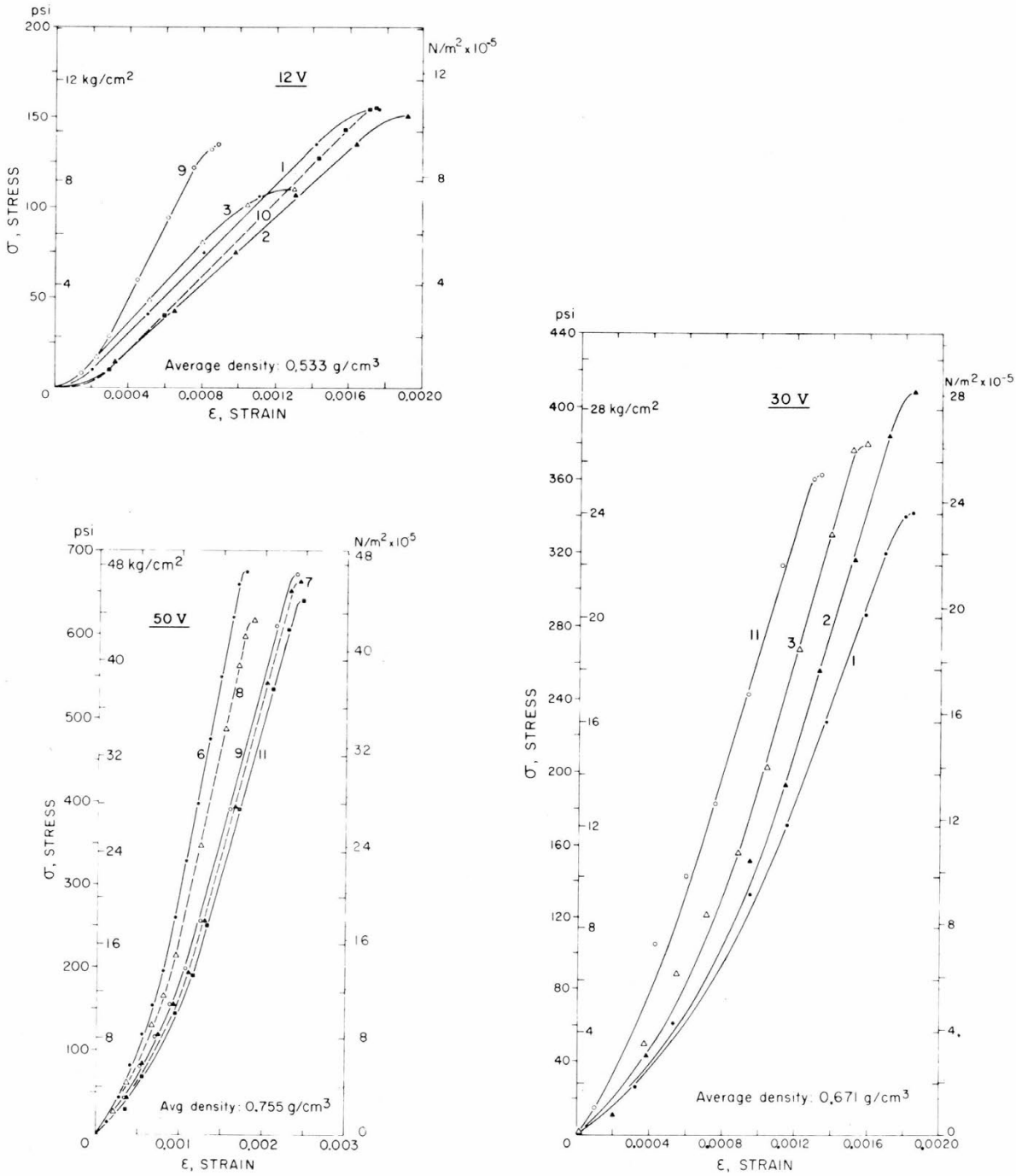

Figure 10. Representative stress-strain curves.

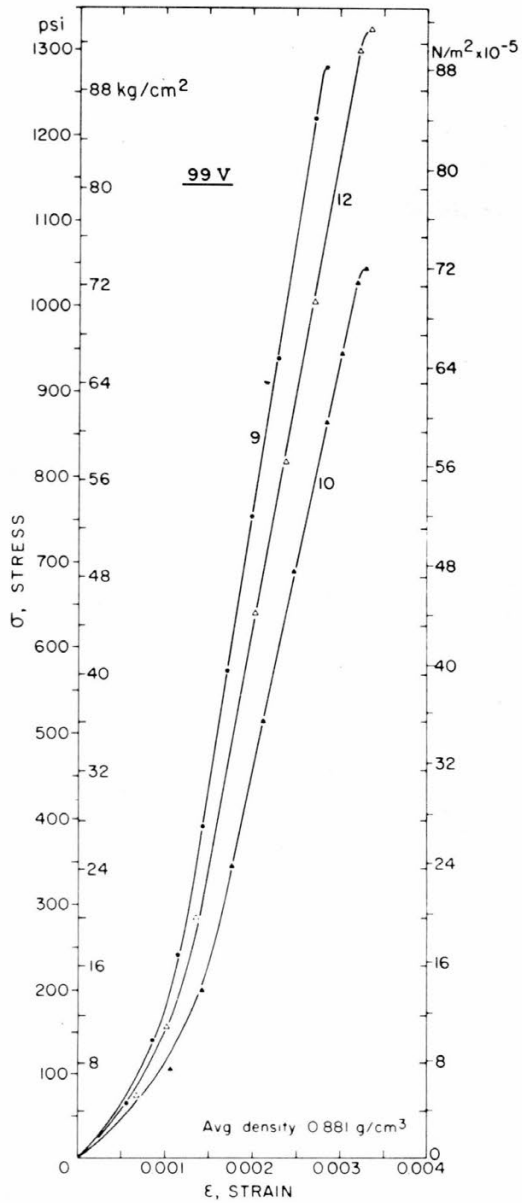

Figure 10 (Cont'd). Representative stress-strain curves.

that this large initial change of the elastic modulus with stress was definitely not the result of seating-in deformation of the equipment. Adams and Williamson (1923) showed that the flaws inherent in a material close under stress. This idea has been widely applied and offers a qualitative explanation for the large initial change in the elastic moduli with stress observed in this study. Another possible reason for this change in slope lies in initial seating deformation of the ice. Because the precise shapes of the curves in this nonlinear region are difficult to ascertain, we do not suggest that initial tangent moduli be determined from these curves. The curvature which appears in the stress-strain curves following the Hookian behavior is typical of mixed mode fracture, due to non-Newtonian viscous deformation at crack tips or the motion of line defects associated with creep.

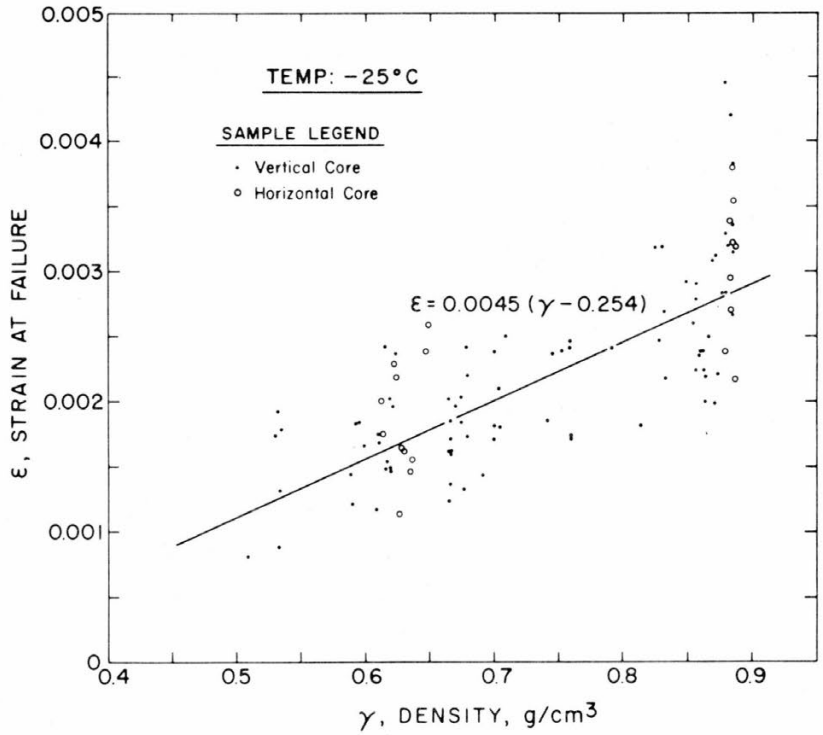

Figure 11. Strain at failure vs density (unconfined compression tests).

Figure 11 graphically shows the linear relation observed between strain at failure and sample density. Isotropic behavior is again manifested by the similar failure strains obtained from horizontally and vertically cored samples of comparable densities when the densities are greater than 0.600 g/cm³.

Young's modulus. The tangent and secant moduli in unconfined compression were obtained from the stress-strain curves and are listed in Appendix B. Modulus values for snow with densities greater than 0.500 g/cm³ are plotted against density in Figure 12. Specimens with densities less than 0.500 g/cm³ are not included in the analysis because as mentioned previously these samples often failed across horizontal planes of weakness, presumably former depth hoar layers. The stresses and strains obtained at failure from these specimens are therefore of questionable value because the true density of the snow that actually failed is not known.

At densities greater than 0.600 g/cm³ isotropic behavior is again indicated inasmuch as both horizontal and vertical specimens give similar relations. The relations between both the tangent and secant moduli and density appear to be linear. An increase in the scatter of the Young's modulus values is again apparent at densities greater than roughly 0.830 g/cm³.

Time effects. The time to failure for each sample is also listed in Appendix B. The values varied between the extremes of 0.2 to 1.4 sec and, as might be expected, showed a systematic increase with increasing density (Fig. 13). Because of a valve malfunction it was not possible to maintain the same ram speed from test to test. Fortunately, however, the ram speed remained constant during individual tests. For the low density samples ($\gamma < 0.620$ g/cm³) ram speeds were as high as 23.6 cm/min. At sample densities higher than this value, the ram speed in general remained close to 8.6 cm/min although occasional fluctuations between 5.1 cm and 9.9 cm/min were noted. Because of these variations no detailed conclusions can be drawn from the shape of the curve in Figure 13.

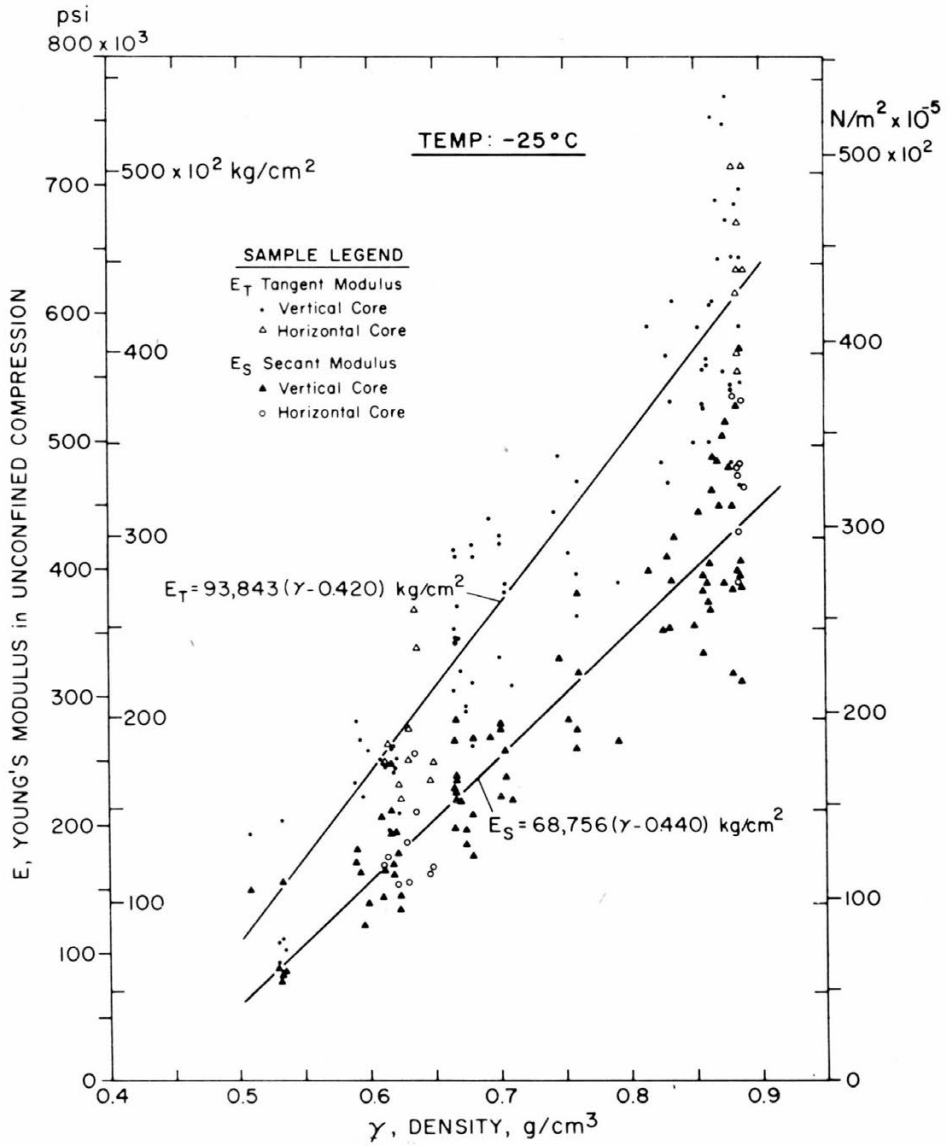

Figure 12. Tangent and secant moduli vs density (unconfined compression tests).

Figure 14 plots the unconfined compressive strength of the samples ($\gamma \geq 0.830$ g/cm³) vs strain rate $\dot{\epsilon}$. Within the $\dot{\epsilon}$ range studied there is no obvious dependency of σ_c on $\dot{\epsilon}$. As would be expected from Figure 9, the higher density specimens give higher failure strengths. Although the lack of dependence of σ_c on $\dot{\epsilon}$ is in agreement with a general rule of thumb used at CRREL ($\sigma_c \neq f(\dot{\epsilon})$ at head speeds above 2.54 cm/min), it is in disagreement with the results of Korzhavin (1962) who found a systematic decrease in the compressive strength of cubes of lake ice as $\dot{\epsilon}$ increased through the same range of values. Results similar to those of Korzhavin have also been reported by Korzhavin and Ptukhin (1966) and Peyton (1966). Direct comparisons, however, are difficult because these authors analyzed their results in terms of stress rates instead of strain rates. Nevertheless their results are quite convincing. It is possible that the differences between our results and those of these authors are produced by changes in the structure of the ice (fine-grained glacier ice as compared with lake and sea ice). This is clearly an area in which further experimentation is needed.

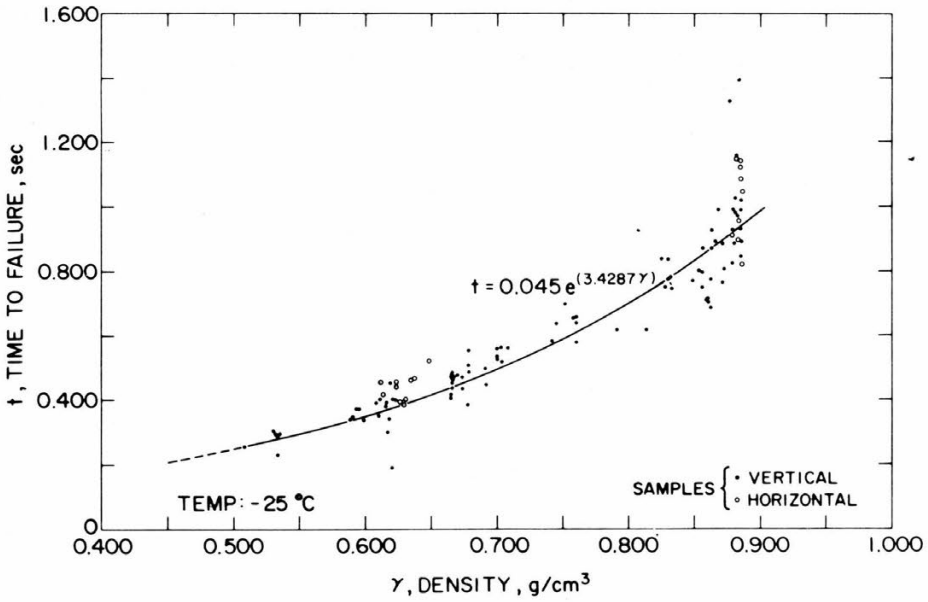

Figure 13. Time to failure vs density (unconfined compression tests).

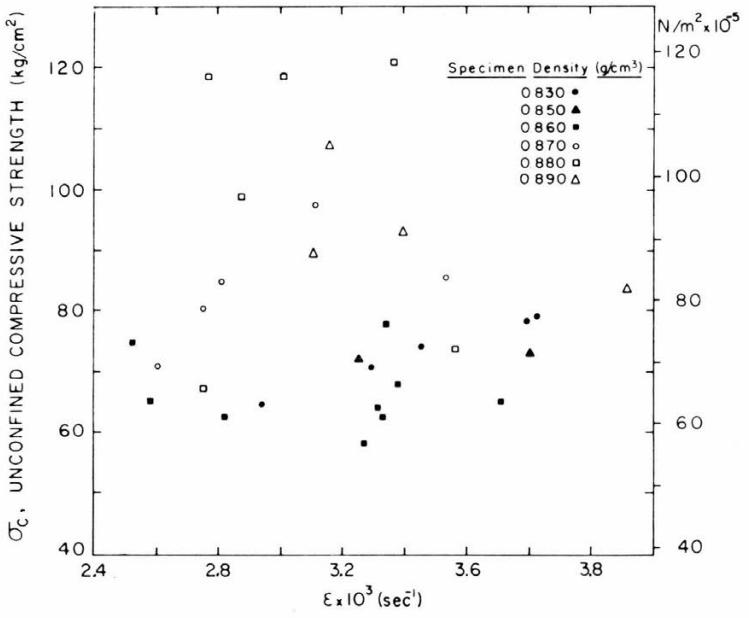

Figure 14. Unconfined compression strength vs strain rate.

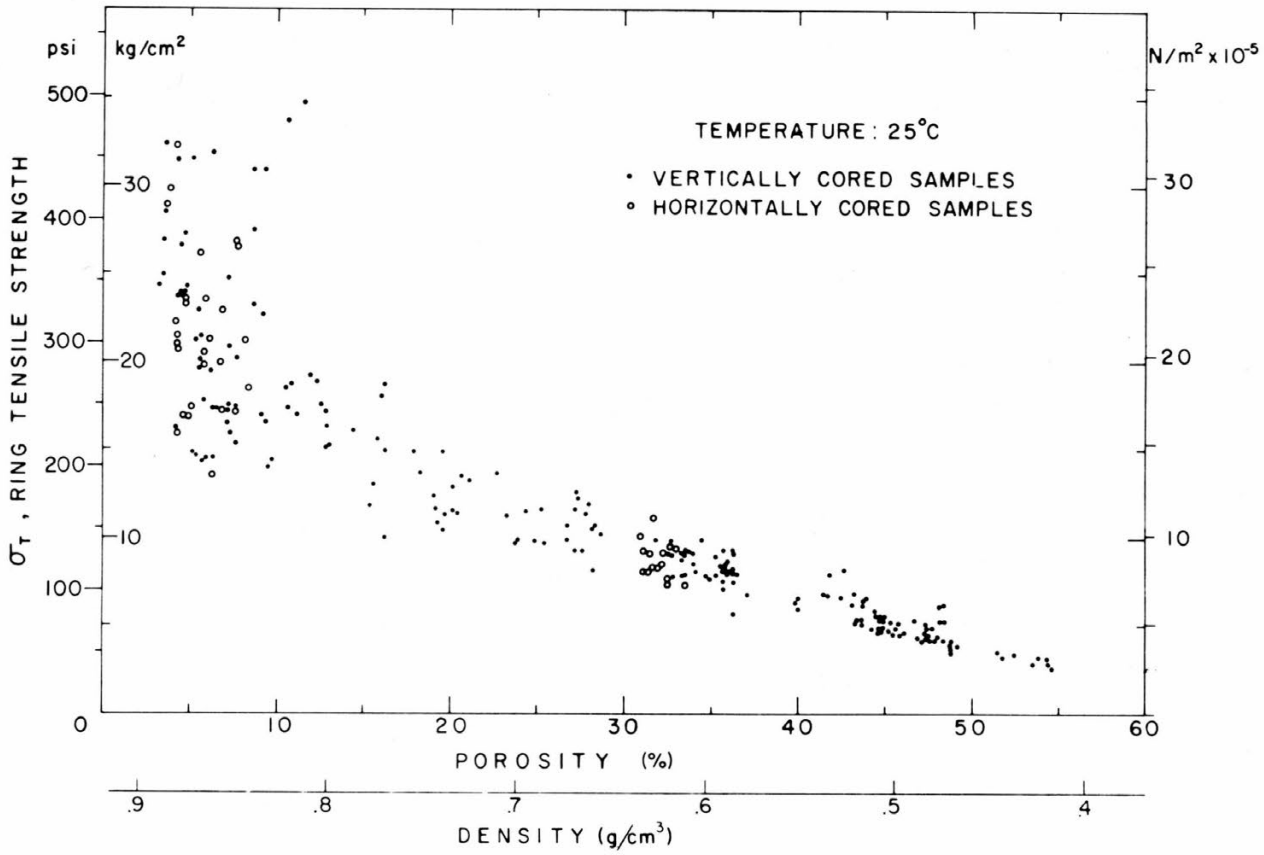

Figure 15. Ring tensile strength vs density and porosity.

Ring tensile tests

Ring tensile test data are listed in Appendix C. Values of the ring tensile strength σ_T are plotted vs sample density and porosity in Figure 15. It is again apparent that at densities greater than 0.600 g/cm³ both horizontally and vertically cored specimens give similar results, indicating isotropic strength behavior. The relation between σ_T and density is essentially linear with a slight but gradual increase in the scatter as density increases from 0.400 to 0.830 g/cm³. For density values higher than 0.830 g/cm³ there is again a pronounced increase in the scatter toward higher strength values.

DISCUSSION

As remarked earlier, considerable care was taken in the present study to produce unconfined compression specimens with ends that were flat, parallel and perpendicular to the axes of the specimens. We believe that it will be difficult under field conditions to significantly improve the quality of the specimens being tested. An attempt was also made to reduce end constraints and to cause rapid failure of the specimens under a constant head speed. These efforts to achieve optimum testing procedures were apparently at least partially successful. Our observed scatter is small for snow and ice unconfined compression results. In short, we believe that the primary cause of scatter in the test data is associated with the singular or combined effects of nonaxially loaded and/or irregularly surfaced specimen ends, and to a lesser degree due to inherent crystalline or

structural flaws. If indeed the scatter is related to the above, then the highest strength values recorded are those obtained from tests in which the samples had most careful preparation and alignment within the testing machine. It then follows that the more realistic unconfined compressive strength vs density relationship would be similar to that indicated by the dashed curve which skirts through the higher strength values in Figure 9.

We were surprised to find that when we corrected our results to –10C using Bender's (1957) temperature correction, our results were, on the average, 18% lower than published results from similar Greenland snow (Kovacs, 1967, Fig. 3: based on data of Butkovich, 1958, and Smith, 1965) and 33% lower than apparently similar Antarctic snow (Ramseier, 1963). There are two possible explanations for this. Possibly Bender's temperature correction is inadequate. Also this decrease may be the result of the high strain rates which were applied to our samples. If the latter is true then our results can be taken to be in overall agreement with the results of Korzhavin (1962) and Korzhavin and Ptukhin (1966) on lake ice and Peyton (1966) on sea ice.

Our ring tensile results are similar in both the low density ($0.450 \leq \gamma \leq 0.700$ g/cm^3, –10C; Butkovich, 1958) and the high density ($0.860 \leq \gamma \leq 0.880$ g/cm^3, –5C; Butkovich, 1959) range to previous results from Greenland. Because the temperature dependence of the ring tensile strength of ice has not been thoroughly studied, these results have not been corrected to a common temperature. This similarity then is a bit surprising inasmuch as the headspeeds during our ring tensile tests were undoubtedly significantly higher than those used by Butkovich and, at least in sea ice studies, increases in headspeed are associated with decreases in ring tensile strengths (Paige and Kennedy, 1967; Weeks and Assur, 1969). This suggests to us that the effect of temperature on ring tensile strength in the range –5C to –25C is probably significant and should be added as a correction before meaningful comparisons are made.

The nonlinearity of the unconfined compressive test results when plotted against density is quite striking. This is in apparent contradiction to the results of several previous investigators (Butkovich, 1958; Smith, 1965; Ramseier, 1963) although Nakaya and Kuroiwa (1967) obtained similar nonlinear results at Site 2. This can easily be explained by the observation that most investigators have had snow of a limited range of densities available for testing. In the range of their data a linear relation quite adequately represented the data. However, when the essentially complete natural density range is examined, the relation is clearly nonlinear.

It is interesting to speculate on possible causes of this nonlinearity. If at a given temperature the strength of snow is governed by the total area of ice bonds per unit area of failure surface, and if the effective porosity on the failure surface n_f is also linear with bulk porosity n, the strength will be a linear function of the density of the specimen (Ballard and McGaw, 1966). This is, of course, provided that the level of internal stress concentration, no matter what its value, is unchanging with density.

In actuality we would expect that, as pointed out by Ballard and McGaw, the ratio n/n_f would gradually increase, approaching 1 as the porosity approaches zero. We would also expect that as the porosity decreases the geometry of the voids would become more regular with the voids, approaching randomly distributed spheres at very low porosities. Because a spherical void will produce a lower stress concentration than irregularly shaped voids, we would expect that if stress concentrations are produced by the voids, the stress concentration will be a maximum in low density and approach a minimum at higher densities. Either of these effects could produce the observed nonlinearity. It should also be remembered that our tests were performed at low temperatures and high strain rates which would minimize any plastic relief at local stress concentrations. However, the density dependence of our ring tensile results was quasi-linear. We would expect that if there were significant changes in the degree of internal stress concentrations it would also be apparent in the ring tensile results. This was not the case.

Another interesting feature of these test results is the apparent increase in scatter at densities close to those of pure ice. This effect is very pronounced in the plot of ring tensile strength vs density (Fig. 15). It also is apparent in the plots of unconfined compressive strength and Young's modulus vs density (Fig. 9 and 12). Examination of these figures suggests that the lower bounds of the data envelopes are continuous up to the highest densities tested. The upper bounds of the data show a similar regular increase until a density of roughly 0.830 g/cm^3 is reached. At densities higher than this value, appreciably higher strength or Young's modulus values are observed than would be expected by extrapolating the upper bound of the data from lower densities. It is natural to associate this effect with the snow-ice transition which is produced by "close-off" of the air bubbles in the ice. This occurs at a bulk density between 0.800 and 0.830 g/cm^3. At densities higher than this, the ice can be considered as a "sealed-cell' material with no communication between the cells.

The increase in the failure strength at densities above the "close-off" density can possibly be explained as follows. It is known from studies of ceramics (Kingery, 1960) that for a given porosity, Young's modulus will be higher for spherical voids than for irregular interconnected voids. This increase in Young's modulus will, therefore, cause an increase in the stress required to produce a given strain at failure.

The problems pointed out by this study are, in the most part, similar to problems encountered in the testing of all types of snow and ice (Kovacs, 1967; Weeks and Assur, 1969). There is an inadequate understanding of the actual failure mechanisms involved. There is also insufficient information on the effects of changes in test conditions such as temperature, sample size and shape and strain rate on the results. Also inadequately understood is how changes in the microstructure of the specimen (grain size, total volume and arrangement of pores, and crystal orientation) affect the observed strengths. To answer these questions careful testing designed to resolve specific questions is required. We believe that the Inclined Drift at Camp Century is an ideal site for such studies inasmuch as it offers uniform, homogeneous snow and ice specimens of almost any density that is required.

LITERATURE CITED

Adams, L.H. and Williamson, E.D. (1923) The compressibility of minerals and rocks at high pressures. *Journal of the Franklin Institute*, vol. 195, p. 475-592.

Anderson, D.L. and Benson, C.S. (1963) The densification and diagenesis of snow. In *Ice and Snow, Properties, Processes and Applications* (W.D. Kingery, ed.). Cambridge, Mass.: The M.I.T. Press, p. 391-411.

Assur, A. (1958) Composition of sea ice and its tensile strength. In *Arctic Sea Ice*, U.S. National Academy of Sciences - National Research Council Publication 598, p. 106-138. Also U.S. Army Snow Ice and Permafrost Research Establishment (USA SIPRE) Research Report 44 (1961), AD 276604.

Ballard, G.E.H. and McGaw, R.W. (1966) A theory of snow failure. In *International Symposium on Scientific Aspects of Snow and Ice Avalanches*. International Association of Scientific Hydrology, Commission of Snow and Ice, Publication no. 69, p. 160-169. Also U.S. Army Cold Regions Research and Engineering Laboratory (USA CRREL) Research Report 137 (1965), AD XL624198.

Bender, J.A. (1957) Testing of a compacted snow runway. American Society of Civil Engineers, *Journal of the Air Transport Division*, vol. 83, no. AT 1, paper 1324.

Butkovich, T.R. (1958) Strength studies of high-density snows. *Transactions, American Geophysical Union*, vol. 39, no. 2, p. 305-312. Also USA SIPRE Research Report 18 (1956), AD 122665.

LITERATURE CITED (Cont'd)

Butkovich, T.R. (1959) Some physical properties of ice from the TUTO Tunnel and Ramp, Thule, Greenland. USA SIPRE Research Report 47, AD 225569.

Kingery, W.D. (1960) *Introduction to ceramics.* New York: J. Wiley and Sons, 781 p.

Korzhavin, K.N. (1962) Vozdeystviie l'da na inzhenernyie sooruzheniia (Action of Ice on Engineering Structures). Novosibirsk: Izdatel'stvo "Nauka" Sibirskoe Otdelenie, 202 p.

_____ and Ptukhin, F.I. (1966) Kotsenke predela prochnosti l'da na szhatie pri kratkovremennykh bystro vozrastaiushchikh nagruzkakh (Evaluating the compressive strength of ice under short-term rapidly increasing loads). Materially VIII Vsesoiuz. mezhduvedomstvennogo soveshchaniia po geokriologiia (merzlotovedeniiu), Vyp. 5, Yakutsk, p. 61-72.

Kovacs, A. (1967) Density, temperature and the unconfined compressive strength of polar snow. USA CRREL Special Report 115.

Langway, C.C. (1967) Stratigraphic analysis of a deep ice core from Greenland. USA CRREL Research Report 77, AD 655264.

Nakaya, U. and Kuroiwa, D. (1967) Physical properties and internal structure of Greenland snow. In *Physics of Snow and Ice,* Sapporo Conference, vol. 1, part 2, p. 953-971.

Paige, R.A. and Kennedy, R.A. (1967) Strength studies of sea ice - effect of load rate on ring tensile strength. U.S. Naval Civil Engineering Laboratory Technical Report R545.

Peyton, H.R. (1966) Sea ice strength. Geophysical Institute of the University of Alaska, Report No. NR 307-247/7-6-55.

Ramseier, R.O. (1963) Some physical and mechanical properties of polar snow. *Journal of Glaciology,* vol. 4, no. 36, p. 753-769. Also USA CRREL Research Report 116 (1966), AD 631685.

Ripperger, E.A. and Davids, N. (1947) Critical stresses in a circular ring. *Proceedings, American Society of Civil Engineers,* vol. 12, p. 619-635.

Smith, J.L. (1965) The elastic constants, strength and density of Greenland snow as determined from measurements of sonic wave velocity. USA CRREL Technical Report 167, AD 632357.

Weeks, W.F. and Assur, A. (1968) The mechanical properties of sea ice. In *Proceedings, Conference on Ice Pressures Against Structures,* (Laval University), National Research Council of Canada, Associate Committee on Geotechnical Research, Technical Memo. No. 92, p. 25-78. Also USA CRREL Cold Regions Science and Engineering Monograph II-C3 (1967), AD 662716.

_____ (1969) Fracture of lake and sea ice. In *Treatise on Fracture* (H. Liebowitz, ed.) New York: Academic Press. Also USA CRREL Research Report 269 (1969).

APPENDIX A. CALCULATION OF THE EFFECT OF NONAXIAL LOADING OF UNCONFINED COMPRESSION SPECIMENS.

The stress distribution (σ) over a uniformly loaded specimen at failure is:

$$\sigma = \frac{P_A}{A} = \frac{P_A}{\pi R^2} \tag{A1}$$

where

P_A = axial load

R = radius of specimen

A = end surface area.

Nonaxial loading reduces the ultimate failure stress by an amount equal to the bending stress (σ_B) which is directly related to the degree of eccentricity e:

$$\sigma_B = \frac{MR}{I} = \frac{4P_E e}{\pi R^3} \tag{A2}$$

where

M = moment, $P_E e$

P_E = eccentric load

I = moment of inertia, $\pi R^4/4$.

If σ is the ultimate stress a uniformly loaded specimen will sustain, a nonuniformly loaded one will therefore support $\sigma - \sigma_B = \sigma_c$ (the observed unconfined compression strength as determined from P_E/A). The percent of reduction in failure strength due to an eccentric loading is then:

$$\frac{\sigma - \sigma_c}{\sigma_c + \sigma_B} = \frac{\sigma_B}{\sigma} \times 100. \tag{A3}$$

From eq A3 the reduction in the failure stress for a 3-in. (7.6-cm) diameter sample subjected to a load applied 0.06 in. (1.5 mm) off center is 14%.

APPENDIX B. CAMP CENTURY UNCONFINED COMPRESSIVE STRENGTH DATA AT −25C.

Snow samples, 8.25 in. (21.0 cm) in length, 3.0 in. (7.6 cm) in diameter. Under Spec. No. the symbol P indicates that the sample was from a surface pit and that its axis was oriented vertically. The symbols H and V indicate that the sample was from the Inclined Drift and had its axis oriented horizontally (H) or vertically (V).

Spec no.	Depth (m)	Depth (ft)	Density (g/cm³)	Press speed (cm/min)	Press speed (in./min)	Time to failure (sec)	Strain at failure	Load at failure (kg)	Load at failure (lb)	Stress at failure (kg/cm²)	Stress at failure (psi)	Secant modulus psi X10³	Secant modulus kg/cm² X10³	Secant modulus dyn/cm² X10¹⁰	Tangent modulus psi X10³	Tangent modulus kg/cm² X10³	Tangent modulus dyn/cm² X10¹⁰
P-1	From surface pit		.516	N/A	N/A	.460	N/A	840	1852	18.66	266	N/A	N/A	N/A	N/A	N/A	N/A
P-2	"	"	"	.443	"	"	.285	"	264	584	5.88	84	"	"	"	"	"	"
P-3	"	"	"	.483	"	"	.305	"	360	796	7.98	114	"	"	"	"	"	"
P-5	"	"	"	.512	"	"	N/A	"	572	1260	12.64	180	"	"	"	"	"	"
P-6	"	"	"	.440	N/A	N/A	.455	N/A	242	536	5.38	76	N/A	N/A	N/A	N/A	N/A	N/A
P-7	"	"	"	.468	23.57	9.28	.330	.00567	294	648	6.54	92	166	11.67	.114	238	16.70	.164
P-8	"	"	"	.438	15.75	6.20	.290	.00476	300	660	6.78	96	202	14.20	.139	455	32.00	.314
P-9	"	"	"	.450	N/A	N/A	.465	N/A	196	432	4.40	62	N/A	N/A	N/A	N/A	N/A	N/A
P-10	"	"	"	.511	"	"	.375	"	720	1588	15.96	228	"	"	"	"	"	"
P-11	"	"	"	.451	"	"	.504	"	250	552	5.58	80	"	"	"	"	"	"
P-12	"	"	"	.343	"	"	N/A	"	64	140	1.46	20	"	"	"	"	"	"
P-13	"	"	"	.417	"	"	.575	"	226	500	5.02	72	"	"	"	"	"	"
P-14	"	"	"	.510	"	"	.385	"	682	1504	15.04	214	"	"	"	"	"	"
P-15	"	"	"	.388	"	"	N/A	"	88	196	1.98	28	"	"	"	"	"	"
P-16	"	"	"	.461	"	"	.240	"	430	948	9.60	136	"	"	"	"	"	"
P-17	"	"	"	.492	"	"	.300	"	498	1100	11.06	158	"	"	"	"	"	"
P-19	"	"	"	.455	"	"	.340	"	438	968	9.72	138	"	"	"	"	"	"
P-20	"	"	"	.509	"	"	.385	"	670	1476	14.84	210	"	"	"	"	"	"
P-21	"	"	"	.480	"	"	.465	"	702	1552	15.52	220	"	"	"	"	"	"
P-25	"	"	"	.422	"	"	N/A	"	246	544	5.50	78	"	"	"	"	"	"
P-26	"	"	"	.418	"	"	.465	"	310	684	6.90	98	N/A	N/A	N/A	N/A	N/A	N/A
P-28	"	"	"	.454	"	"	.365	.00602	680	1500	15.20	216	359	25.25	.248	691	48.59	.477
P-29	"	"	"	.451	"	"	.370	N/A	490	1080	10.92	156	N/A	N/A	N/A	N/A	N/A	N/A
P-30	"	"	"	.513	"	"	.375	"	344	760	7.64	108	"	"	"	"	"	"
P-31	"	"	"	.443	"	"	.352	"	296	652	6.56	94	"	"	"	"	"	"
P-32	"	"	"	.518	N/A	N/A	.340	N/A	596	1312	13.16	188	N/A	N/A	N/A	N/A	N/A	N/A
P-33	"	"	"	.431	21.44	8.44	.320	.00581	320	704	7.20	102	176	12.38	.121	429	30.17	.296
P-34	"	"	"	.502	N/A	N/A	.285	N/A	474	1044	10.50	150	N/A	N/A	N/A	N/A	N/A	N/A
P-35	"	"	"	.441	"	"	.480	"	498	1100	11.24	160	"	"	"	"	"	"
P-36	"	"	"	.506	"	"	.315	"	536	1184	11.90	170	"	"	"	"	"	"
P-37	"	"	"	.511	N/A	N/A	.350	N/A	506	1116	11.22	160	N/A	N/A	N/A	N/A	N/A	N/A
P-38	From surface pit		.480	N/A	N/A	.340	N/A	526	1160	11.70	166	N/A	N/A	N/A	N/A	N/A	N/A
P-39	"	"	"	.417	"	"	N/A	"	228	504	5.14	72	"	"	"	"	"	"
P-40	"	"	"	.497	"	"	N/A	"	442	976	9.82	140	"	"	"	"	"	"
P-42	"	"	"	.470	"	"	.385	"	448	988	9.94	142	"	"	"	"	"	"
P-43	"	"	"	.517	"	"	.340	"	620	1368	13.76	196	"	"	"	"	"	"
P-44	"	"	"	.511	"	"	.315	"	482	1064	10.70	152	"	"	"	"	"	"
P-45	"	"	"	.437	"	"	.210	"	206	456	4.64	66	"	"	"	"	"	"
P-46	"	"	"	.509	"	"	.360	"	650	1432	14.40	204	"	"	"	"	"	"
P-47	"	"	"	.382	"	"	N/A	"	118	260	2.68	38	"	"	"	"	"	"
P-48	"	"	"	.444	"	"	.310	"	576	1052	10.72	152	"	"	"	"	"	"
P-49	"	"	"	.528	"	"	.465	"	1014	2236	22.48	320	"	"	"	"	"	"
P-50	"	"	"	.454	"	"	.240	"	454	1000	10.14	144	"	"	"	"	"	"
P-51	"	"	"	.471	"	"	.280	"	412	910	9.30	132	"	"	"	"	"	"
P-52	"	"	"	.517	"	"	N/A	"	340	750	7.50	106	"	"	"	"	"	"
P-54	"	"	"	.474	"	"	.235	"	300	660	6.66	94	"	"	"	"	"	"
P-55	"	"	"	.477	"	"	N/A	"	404	890	8.98	128	"	"	"	"	"	"
P-56	"	"	"	.508	"	"	.280	"	476	1050	10.56	150	"	"	"	"	"	"
P-57	"	"	"	.496	"	"	.240	"	544	1200	12.06	172	"	"	"	"	"	"
P-59	"	"	"	.503	"	"	.210	"	454	1000	10.06	142	"	"	"	"	"	"
P-60	"	"	"	.473	"	"	.175	"	318	700	7.04	100	"	"	"	"	"	"
P-61	"	"	"	.481	"	"	.150	"	386	850	8.54	122	"	"	"	"	"	"
P-62	"	"	"	.441	"	"	N/A	"	250	550	5.62	80	"	"	"	"	"	"
P-63	"	"	"	.376	"	"	N/A	"	90	200	2.12	30	"	"	"	"	"	"
P-65	"	"	"	.385	N/A	N/A	N/A	N/A	136	306	3.08	44	N/A	N/A	N/A	N/A	N/A	N/A
P-66	"	"	"	.456	23.32	9.18	.295	.00550	422	930	9.34	132	240	16.88	.166	321	22.57	.221
P-67	"	"	"	.503	N/A	N/A	.300	N/A	508	1120	11.20	160	N/A	N/A	N/A	N/A	N/A	N/A
P-68	"	"	"	.478	"	"	.385	"	376	830	8.34	118	"	"	"	"	"	"
P-69	"	"	"	.368	"	"	N/A	"	46	100	1.02	14	"	"	"	"	"	"
P-70	"	"	"	.466	"	"	N/A	"	372	820	8.24	118	"	"	"	"	"	"
P-71	"	"	"	.432	"	"	N/A	"	272	600	6.10	86	"	"	"	"	"	"
P-73	"	"	"	.481	N/A	N/A	.230	N/A	294	650	6.50	92	N/A	N/A	N/A	N/A	N/A	N/A

Spec no.	Depth (m)	Depth (ft)	Density (g/cm³)	Press speed (cm/min)	Press speed (in./min)	Time to failure (sec)	Strain at failure	Load at failure (kg)	Load at failure (lb)	Stress at failure (kg/cm²)	Stress at failure (psi)	Secant modulus psi X10²	Secant modulus kg/cm² X10²	Secant modulus dyn/cm² X10¹⁰	Tangent modulus psi X10²	Tangent modulus kg/cm² X10²	Tangent modulus dyn/cm² X10¹⁰
P-74	From surface pit		.431	19.63	7.73	.260	.00378	340	750	7.70	110	299	21.03	.206	495	34.81	.341
P-75	"	"	.515	N/A	N/A	.265	N/A	444	980	9.80	140	N/A	N/A	N/A	N/A	N/A	N/A
P-76	"	"	.394	"	"	N/A	"	68	150	1.44	22	"	"	"	"	"	"
P-77	"	"	.462	"	"	"	"	208	460	4.64	66	"	"	"	"	"	"
P-79	"	"	.494	"	"	"	"	612	1350	13.56	192	"	"	"	"	"	"
P-80	"	"	.424	"	"	"	"	190	420	4.28	60	"	"	"	"	"	"
P-81	"	"	.432	"	"	"	"	272	600	6.02	86	"	"	"	"	"	"
P-82	"	"	.439	N/A	N/A	N/A	N/A	208	460	4.64	66	N/A	N/A	N/A	N/A	N/A	N/A
P-83	"	"	.462	17.78	7.00	.225	.00301	412	910	9.22	132	439	30.87	.303	664	46.49	.458
P-84	"	"	.488	N/A	N/A	.320	N/A	576	1270	12.74	180	N/A	N/A	N/A	N/A	N/A	N/A
P-85	"	"	.466	18.87	7.43	.265	.00361	318	700	7.12	102	283	19.90	.195	500	35.16	.346
P-86	"	"	.501	N/A	N/A	.555	N/A	748	1650	16.58	234	N/A	N/A	N/A	N/A	N/A	N/A
P-87	"	"	.457	"	"	.315	"	354	780	7.90	112	"	"	"	"	"	"
P-88	"	"	.472	"	"	.375	"	394	870	8.82	126	"	"	"	"	"	"
P-89	"	"	.504	N/A	N/A	N/A	N/A	666	1470	14.90	212	N/A	N/A	N/A	N/A	N/A	N/A
P-90	"	"	.477	18.87	7.43	.396	.00400	494	1090	10.98	156	391	27.50	.270	742	52.18	.512
P-91	"	"	.439	N/A	N/A	.310	N/A	172	380	3.86	54	N/A	N/A	N/A	N/A	N/A	N/A
P-92	"	"	.473	"	"	N/A	"	190	420	4.22	60	"	"	"	"	"	"
P-93	"	"	.444	"	"	N/A	"	276	610	6.22	88	"	"	"	"	"	"
P-94	"	"	.491	"	"	.300	"	498	1100	11.08	158	"	"	"	"	"	"
P-95	"	"	.479	"	"	.400	"	412	910	9.18	130	"	"	"	"	"	"
P-96	"	"	.485	"	"	N/A	"	318	700	7.06	100	"	"	"	"	"	"
P-97	"	"	.452	"	"	"	"	240	530	5.36	76	"	"	"	"	"	"
P-98	"	"	.445	"	"	"	"	322	710	7.20	102	"	"	"	"	"	"
P-99	"	"	.438	"	"	N/A	"	262	580	5.96	84	"	"	"	"	"	"
P-100	"	"	.457	"	"	.230	"	430	950	9.60	136	"	"	"	"	"	"
P-101	"	"	.437	"	"	N/A	"	250	550	5.62	80	"	"	"	"	"	"
P-102	"	"	.451	"	"	N/A	"	444	980	10.06	142	"	"	"	"	"	"
P-103	"	"	.441	"	"	N/A	"	176	390	3.94	56	"	"	"	"	"	"
P-104	"	"	.447	N/A	N/A	.295	N/A	268	590	5.94	84	N/A	N/A	N/A	N/A	N/A	N/A
12V-1	12	39	.535	12.06	4.75	.295	.00178	481	1080	10.80	154	866	60.90	.597	1030	72.43	.711
12V-2	12	39	.532	12.01	4.73	.295	.00192	354	1060	10.61	151	787	55.34	.543	930	65.40	.642
12V-3	12	39	.534	11.33	4.46	.230	.00131	354	780	7.80	110	840	59.07	.580	1120	78.76	.773
12V-4	12	39	.525	N/A	N/A	.255	N/A	N/A	N/A	N/A	N/A	N/A	N/A	N/A	N/A	N/A	N/A
12V-5	12	39	.525	N/A	N/A	.205	N/A	N/A	N/A	N/A	N/A	N/A	N/A	N/A	N/A	N/A	N/A
12V-6	12	39	.508	8.97	3.54	.255	.00081	386	850	8.50	121	680	47.82	.469	830	58.37	.572
12V-7	12	39	.529	N/A	N/A	.225	N/A	N/A	N/A	N/A	N/A	N/A	N/A	N/A	N/A	N/A	N/A
12V-8	12	39	.536	N/A	N/A	.280	N/A	N/A	N/A	N/A	N/A	N/A	N/A	N/A	N/A	N/A	N/A
12V-9	12	39	.533	9.78	3.85	.290	.00088	431	950	9.50	135	1530	107.60	1.056	2040	143.46	1.408
12V-10	12	39	.530	9.22	3.63	.305	.00174	490	1080	10.80	154	885	62.23	.611	1080	75.95	.745
12V-12	12	39	.536	N/A	N/A	.255	N/A	N/A	N/A	N/A	N/A	N/A	N/A	N/A	N/A	N/A	N/A
12V-13	12	39	.527	"	"	.240	"	"	"	"	"	"	"	"	"	"	"
12V-14	12	39	.526	"	"	.180	"	"	"	"	"	"	"	"	"	"	"
20V-1	20	66	.621	"	"	.445	"	"	"	"	"	"	"	"	"	"	"
20V-2	20	66	.622	"	"	.375	"	"	"	"	"	"	"	"	"	"	"
20V-3	20	66	.612	N/A	N/A	.425	N/A	N/A	N/A	N/A	N/A	N/A	N/A	N/A	N/A	N/A	N/A
20V-4	20	66	.608	7.49	2.95	.300	.00117	771	1700	21.50	242	2070	145.57	1.428	2520	177.22	1.739
20V-6	20	66	.619	10.57	4.16	.450	.00202	1043	2300	23.00	327	1620	113.92	1.118	2420	170.18	1.670
20V-7	20	66	.617	N/A	N/A	.415	N/A	N/A	N/A	N/A	N/A	N/A	N/A	N/A	N/A	N/A	N/A
20V-8	20	66	.608	N/A	N/A	.360	"	"	"	"	"	"	"	"	"	"	"
20V-9	20	66	.604	N/A	N/A	.430	N/A	N/A	N/A	N/A	N/A	N/A	N/A	N/A	N/A	N/A	N/A
20V-10	20	66	.611	9.02	3.55	.400	.00168	889	1960	19.60	279	1660	116.74	1.145	2460	173.00	1.697
20V-11	20	66	.622	N/A	N/A	.330	N/A	N/A	N/A	N/A	N/A	N/A	N/A	N/A	N/A	N/A	N/A
20V-12	20	66	.617	N/A	N/A	.375	N/A	N/A	N/A	N/A	N/A	N/A	N/A	N/A	N/A	N/A	N/A
20V-15	20	66	.588	8.64	3.40	.340	.00144	790	1740	17.41	248	1720	120.96	1.187	2340	164.56	1.615
20V-33	20	66	.617	12.37	4.87	.300	.00154	1043	2300	23.00	327	2120	149.09	1.463	2600	182.84	1.794
20V-34	20	66	.620	16.51	6.50	.190	.00147	916	2020	20.20	287	1950	137.13	1.345	2450	172.29	1.690
20V-35	20	66	.610	11.02	4.34	.350	.00175	807	1780	17.80	253	1450	101.97	1.000	2480	174.41	1.711
20V-37	20	66	.623	12.80	5.04	.400	.00237	1020	2250	22.50	320	1350	94.94	.931	2100	147.68	1.449
20V-38	20	66	.609	N/A	N/A	N/A	N/A	N/A	N/A	N/A	N/A	N/A	N/A	N/A	N/A	N/A	N/A
20V-39	20	66	.618	10.18	4.01	.340	.00149	807	1780	17.80	253	1700	119.55	1.173	2642	185.65	1.822

Spec no.	Depth (m)	Depth (ft)	Density (g/cm³)	Press speed (cm/min)	Press speed (in./min)	Time to failure (sec)	Strain at failure	Load at failure (kg)	Load at failure (lb)	Stress at failure (kg/cm²)	Stress at failure (psi)	Secant modulus psi X10²	Secant modulus kg/cm² X10²	Secant modulus dyn/cm² X10¹⁰	Tangent modulus psi X10²	Tangent modulus kg/cm² X10²	Tangent modulus dyn/cm² X10¹⁰
20V-40	20	66	.615	12.22	4.81	.380	.00242	912	2010	20.10	286	1180	82.98	.814	1970	138.54	1.359
20V-41	20	66	.599	9.37	3.69	.335	.00166	744	1640	16.40	233	1400	98.45	.966	2580	181.44	1.780
20V-42	20	66	.616	N/A	N/A	N/A	N/A	N/A	N/A	N/A	N/A	N/A	N/A	N/A	N/A	N/A	N/A
20V-44	20	66	.595	11.18	4.40	.365	.00184	721	1590	15.90	226	1230	86.50	.849	2230	156.82	1.539
20V-45	20	66	.603	N/A	N/A	N/A	N/A	N/A	N/A	N/A	N/A	N/A	N/A	N/A	N/A	N/A	N/A
20V-46	20	66	.595	"	"	"	"	"	"	"	"	"	"	"	"	"	"
20V-47	20	66	.622	"	"	"	"	"	"	"	"	"	"	"	"	"	"
20V-48	20	66	.595	N/A	N/A	N/A	N/A	N/A	N/A	N/A	N/A	N/A	N/A	N/A	N/A	N/A	N/A
20V-50	20	66	.621	11.02	4.34	.400	.00197	1116	2460	24.60	350	1780	125.18	1.228	2520	177.22	1.738
20V-51	20	66	.593	11.30	4.45	.370	.00178	930	2050	20.50	292	1640	115.33	1.125	2670	187.76	1.842
20V-52	20	66	.616	9.09	3.58	.390	.00148	916	2020	20.20	287	1940	136.43	1.339	2480	174.40	1.711
20V-53	20	66	.590	9.24	3.64	.348	.00121	698	1540	15.40	219	1810	127.29	1.250	2820	198.31	1.946
30V-1	30	98	.674	9.50	3.74	.435	.00184	1093	2410	24.10	343	1860	130.80	1.283	2880	202.53	1.987
30V-2	30	98	.666	8.61	3.39	.485	.00185	1302	2870	28.70	408	2200	154.71	1.518	3460	243.32	2.387
30V-3	30	98	.667	9.17	3.61	.470	.00159	1211	2670	26.70	380	2390	168.07	1.649	3710	260.90	2.560
30V-4	30	98	.669	N/A	N/A	.500	N/A	1388	3060	30.60	435	N/A	N/A	N/A	N/A	N/A	N/A
30V-5	30	98	.679	8.48	3.34	.546	.00173	1479	3260	32.60	464	2680	188.47	1.849	4100	288.33	2.829
30V-6	30	98	.665	8.81	3.47	.475	.00162	1179	2600	26.00	370	2290	161.04	1.580	3530	161.04	1.580
30V-7	30	98	.678	9.19	3.62	.505	.00242	1370	3020	30.20	429	1770	124.47	1.221	2620	184.25	1.808
30V-8	30	98	.666	8.43	3.32	.435	.00136	1225	2700	27.00	384	2820	198.31	1.946	4100	198.31	1.946
30V-9	30	98	.666	7.95	3.13	.450	.00162	1170	2580	25.80	367	2260	158.93	1.559	3450	158.93	1.559
30V-10	30	98	.674	9.91	3.90	.470	.00203	1274	2810	28.10	400	1970	138.54	1.359	2930	138.54	1.359
30V-11	30	98	.677	8.81	3.47	.385	.00132	1157	2550	25.50	363	2750	193.39	1.897	4180	293.95	2.884
30V-12	30	98	.670	9.47	3.73	.475	.00196	1365	3010	30.10	428	2180	153.30	1.504	3200	225.04	2.208
30V-13	30	98	.679	9.30	3.66	.485	.00220	1467	3230	32.30	460	2090	146.98	1.442	3110	218.71	2.146
30V-14	30	98	.666	9.35	3.68	.460	.00172	1293	2850	28.50	405	2360	165.96	1.628	3420	240.51	2.360
30V-15	30	98	.675	N/A	N/A	.365	N/A	1463	3225	32.25	459	N/A	N/A	N/A	N/A	N/A	N/A
30V-16	30	98	.665	9.40	3.70	.475	.00202	1279	2820	28.20	401	1986	139.94	1.373	3050	214.49	2.104
37V-1	37	121	.704	9.40	3.70	.515	.00180	1370	3020	30.20	429	2380	167.37	1.642	3890	273.56	2.684
37V-2	37	121	.700	N/A	N/A	.580	N/A	1610	3550	35.50	505	N/A	N/A	N/A	N/A	N/A	N/A
37V-3	37	121	.665	6.91	2.72	.415	.00124	1052	2320	23.20	330	2660	187.06	1.835	4150	291.84	2.864
37V-4	37	121	.665	7.49	2.95	.404	N/A	1052	2320	23.20	330	N/A	N/A	N/A	N/A	N/A	N/A
37V-5	37	121	.692	8.56	3.37	.445	.00143	1229	2710	27.10	385	2690	189.17	1.856	4400	309.42	3.036
37V-6	37	121	.691	8.30	3.27	.495	N/A	1492	3290	32.90	468	N/A	N/A	N/A	N/A	N/A	N/A
37V-7	37	121	.700	6.96	2.74	.533	.00181	1597	3520	35.20	501	2770	194.80	1.911	4200	295.36	2.898
37V-8	37	121	.709	9.68	3.81	.560	.00252	1746	3850	38.50	549	2200	154.71	1.518	3090	217.30	2.132
37V-9	37	121	.708	N/A	N/A	.575	N/A	1814	4000	40.00	569	N/A	N/A	N/A	N/A	N/A	N/A
37V-10	37	121	.703	N/A	N/A	.550	N/A	1678	3700	37.00	526	N/A	N/A	N/A	N/A	N/A	N/A
37V-11	37	121	.700	9.80	3.86	.555	.00238	1690	3730	37.30	531	2230	156.81	1.539	3310	232.77	2.284
37V-12	37	121	.700	8.69	3.42	.525	.00171	1519	3350	33.50	476	2780	195.50	1.918	4270	300.28	2.946
37V-13	37	121	.703	9.80	3.86	.560	.00210	2182	3810	38.10	541	2580	181.44	1.780	3820	268.64	2.636
37V-14	37	121	.721	N/A	N/A	.425	N/A	1365	3010	30.10	428	N/A	N/A	N/A	N/A	N/A	N/A
37V-15	37	121	.727	"	"	.465	"	1610	3550	35.50	505	"	"	"	"	"	"
50V-1	50	164	.755	"	"	N/A	"	2182	4810	48.10	684	"	"	"	"	"	"
50V-2	50	164	.765	"	"	.650	"	1905	4200	42.00	597	"	"	"	"	"	"
50V-3	50	164	.758	"	"	.650	"	2009	4430	44.30	630	"	"	"	"	"	"
50V-4	50	164	.740	N/A	N/A	.675	N/A	2023	4460	44.60	634	N/A	N/A	N/A	N/A	N/A	N/A
50V-6	50	164	.760	7.04	2.77	.659	.00177	2154	4750	47.50	675	3820	268.64	2.636	5500	386.78	3.795
50V-7	50	164	.655	7.47	2.94	.655	.00241	2114	4660	46.60	663	2750	193.39	1.898	3970	279.18	2.739
50V-8	50	164	.745	8.41	3.31	.635	.00187	1964	4330	43.30	616	3300	232.07	2.277	4890	343.88	3.374
50V-9	50	164	.752	8.61	3.39	.697	.00238	2140	4720	47.20	671	2820	198.31	1.946	4130	290.44	2.850
50V-10	50	164	.787	N/A	N/A	.685	N/A	2335	5150	51.50	732	N/A	N/A	N/A	N/A	N/A	N/A
50V-11	50	164	.758	9.07	3.57	.635	.00246	2041	4500	45.00	640	2600	182.84	1.794	3640	255.98	2.512
50V-12	50	164	.760	8.36	3.29	.575	.00171	1737	3830	38.30	545	3190	224.43	2.201	4680	329.11	3.229
50V-13	50	164	.742	8.33	3.28	.580	.00185	1769	3900	39.00	555	3000	210.97	2.070	4450	312.94	3.070
57V-1	57	187	.796	N/A	N/A	.745	N/A	2771	6110	61.10	869	N/A	N/A	N/A	N/A	N/A	N/A
57V-2	57	187	.791	9.22	3.63	.615	.00242	2048	4520	45.20	643	2660	187.06	1.835	3900	274.26	2.691
57V-3	57	187	.810	N/A	N/A	.770	N/A	3039	6700	67.00	953	N/A	N/A	N/A	N/A	N/A	N/A
57V-4	57	187	.796	"	"	.550	"	2100	4630	46.30	658	"	"	"	"	"	"
57V-5	57	187	.809	"	"	.660	"	2545	5610	56.25	800	"	"	"	"	"	"
57V-6	57	187	.797	"	"	.600	"	2767	6100	61.00	868	"	"	"	"	"	"
57V-7	57	187	.775	N/A	N/A	.600	N/A	2302	5075	50.75	722	N/A	N/A	N/A	N/A	N/A	N/A

Spec no.	Depth (m)	Depth (ft)	Density (g/cm³)	Press speed (cm/min)	Press speed (in./min)	Time to failure (sec)	Strain at failure	Load at failure (kg)	Load at failure (lb)	Stress at failure (kg/cm²)	Stress at failure (psi)	Secant modulus psi X10³	Secant modulus kg/cm² X10³	Secant modulus dyn/cm² X10¹⁰	Tangent modulus psi X10³	Tangent modulus kg/cm² X10³	Tangent modulus dyn/cm² X10¹⁰
57V-8	57	187	.777	N/A	N/A	.550	N/A	1987	4380	43.80	623	N/A	N/A	N/A	N/A	N/A	N/A
57V-9	57	187	.814	8.43	3.32	.615	.00181	2304	5080	50.80	723	3990	280.59	2.753	5900	414.90	4.071
57V-10	57	187	.790	N/A	N/A	.680	N/A	2612	5760	57.75	821	N/A	N/A	N/A	N/A	N/A	N/A
57V-11	57	187	.805	"	"	.685	"	2536	5590	55.75	793	"	"	"	"	"	"
57V-12	57	187	.790	"	"	.660	"	2490	5490	54.90	781	"	"	"	"	"	"
57V-13	57	187	.776	"	"	.605	"	2041	4500	45.00	640	"	"	"	"	"	"
57V-14	57	187	.778	"	"	.655	"	2368	5220	52.20	742	"	"	"	"	"	"
57V-15	57	187	.807	N/A	N/A	.679	"	2177	4800	48.00	683	"	"	"	"	"	"
72V-1	72	236	.830	8.38	3.30	.830	N/A	3257	7180	71.80	1021	N/A	N/A	N/A	N/A	N/A	N/A
72V-2	72	236	.833	8.61	3.39	.745	.00219	2930	6460	64.60	919	4250	298.88	2.932	6100	428.97	4.209
72V-3	72	236	.832	N/A	N/A	N/A	N/A	2985	6580	65.80	936	N/A	N/A	N/A	N/A	N/A	N/A
72V-4	72	236	.828	8.46	3.33	.750	.00247	3220	7100	71.00	1010	4100	288.33	2.829	5670	398.73	3.912
72V-5	72	236	.825	9.75	3.84	.839	.00318	3561	7850	78.50	1120	3520	247.54	2.429	4840	340.37	3.340
72V-6	72	236	.830	9.75	3.84	.835	.00319	3601	7940	79.40	1129	3540	248.94	2.443	4680	329.11	3.229
72V-7	72	236	.832	9.04	3.56	.780	.00269	3352	7390	73.90	1051	3910	274.97	2.698	5310	373.42	3.664
72V-9	72	236	.830	N/A	N/A	.725	N/A	2767	6100	61.00	867	N/A	N/A	N/A	N/A	N/A	N/A
72V-10	72	236	.827	"	"	N/A	"	2767	6100	61.00	867	"	"	"	"	"	"
72V-11	72	236	.831	"	"	.750	"	2626	5790	57.90	823	"	"	"	"	"	"
72V-13	72	236	.834	"	"	.725	"	2708	5970	59.70	849	"	"	"	"	"	"
72V-14	72	236	.844	N/A	N/A	.680	N/A	2385	5260	52.60	748	N/A	N/A	N/A	N/A	N/A	N/A
80V-1	80	262	.859	8.84	3.48	.710	.00235	2907	6410	64.10	912	3890	273.56	2.684	5650	397.33	3.898
80V-3	80	262	.860	9.19	3.62	.715	.00238	2846	6275	62.75	892	3750	263.71	2.588	5600	393.81	3.864
80V-4	80	262	.853	9.02	3.55	.800	.00260	3266	7200	72.00	1024	3940	277.07	2.719	5900	414.91	4.071
80V-9	80	262	.852	9.32	3.67	.600	N/A	2858	6300	63.00	898	N/A	N/A	N/A	N/A	N/A	N/A
80V-11	80	262	.861	9.73	3.83	.704	.00238	3084	6800	68.00	967	4050	284.81	2.794	5000	351.62	3.450
80V-15	80	262	.849	N/A	N/A	.675	N/A	2685	5920	59.35	844	N/A	N/A	N/A	N/A	N/A	N/A
80V-16	80	262	.849	7.11	2.80	.769	.00292	3311	7300	73.00	1038	3560	250.35	2.456	5000	351.62	3.450
85V-1	85	279	.880	N/A	N/A	.800	N/A	3300	7275	73.13	1040	N/A	N/A	N/A	N/A	N/A	N/A
85V-2	85	279	.873	8.76	3.45	.805	.00221	3640	8025	80.25	1141	5170	363.57	3.567	7700	541.49	5.313
85V-3	85	279	.856	8.76	3.45	.869	.00290	3515	7755	77.70	1105	3820	286.64	2.636	5560	391.00	3.836
85V-4	85	279	.862	8.76	3.45	.685	.00224	2635	5800	58.00	825	3680	258.79	2.539	6070	426.86	4.188
85V-5	85	279	.870	N/A	N/A	.867	N/A	3254	7175	71.75	1020	N/A	N/A	N/A	N/A	N/A	N/A
85V-6	85	279	.871	8.51	3.35	.764	.00199	3209	7075	70.93	1008	5050	355.13	3.484	7490	526.72	5.168
85V-7	85	279	.863	8.05	3.17	.775	.00200	2948	6500	65.00	924	4620	324.90	3.188	7530	529.54	5.196
85V-8	85	279	.863	8.61	3.39	.925	N/A	4105	9050	90.50	1287	N/A	N/A	N/A	N/A	N/A	N/A
85V-9	85	279	.866	8.66	3.41	.890	.00250	3850	8490	84.90	1211	4850	341.07	3.346	6890	484.53	4.754
85V-10	85	279	.868	8.86	3.49	.989	.00308	4400	9700	97.51	1387	4500	316.46	3.105	6430	452.18	4.437
85V-11	85	279	.872	9.35	3.68	.884	.00312	3855	8500	85.22	1212	3900	274.26	2.691	5550	390.30	3.830
85V-12	85	279	.856	9.55	3.76	.750	.00278	2957	6520	65.20	927	3340	234.88	2.305	5270	370.60	3.636
85V-14	85	279	.856	7.62	3.00	.794	.00284	2821	6225	62.25	888	3960	278.48	2.732	5300	372.71	3.657
85V-16	85	279	.863	7.06	2.78	.869	.00219	3390	7475	74.75	1066	4880	343.18	3.367	6100	428.97	4.209
99V-1	99	325	.883	N/A	N/A	1.365	N/A	3592	7920	79.40	1129	N/A	N/A	N/A	N/A	N/A	N/A
99V-3	99	325	.883	"	"	N/A	"	4636	10220	102.46	1457	"	"	"	"	"	"
99V-4	99	325	.878	N/A	N/A	N/A	N/A	5114	11215	112.15	1650	N/A	N/A	N/A	N/A	N/A	N/A
99V-5	99	325	.878	8.33	3.28	1.329	.00446	5490	12100	121.00	1716	3850	270.74	2.656	5430	381.86	3.747
99V-6	99	325	.885	8.71	3.43	1.017	.00315	4071	8975	89.75	1276	4060	285.51	2.801	5910	415.61	4.078
99V-7	99	325	.887	N/A	N/A	1.040	N/A	3969	8750	87.96	1251	N/A	N/A	N/A	N/A	N/A	N/A
99V-8	99	325	.883	N/A	N/A	.975	N/A	4003	8825	88.50	1258	N/A	N/A	N/A	N/A	N/A	N/A
99V-9	99	325	.879	7.67	3.02	.989	.00284	4082	9000	90.90	1280	4500	316.46	3.105	6450	453.59	4.450
99V-10	99	325	.879	8.56	3.37	.924	.00329	3334	7350	73.50	1045	3180	223.63	2.194	4850	341.07	3.346
99V-11	99	325	.881	8.18	3.22	1.159	.00320	5375	11850	118.50	1685	5280	371.31	3.650	6860	482.42	4.733
99V-12	99	325	.885	8.56	3.37	.989	.00336	4230	9325	93.25	1326	3950	277.78	2.726	6450	453.59	4.450
99V-13	99	325	.885	9.14	3.60	.929	.00382	3799	8375	83.75	1191	3120	219.41	2.153	4670	328.41	3.222
99V-15	99	325	.886	9.65	3.80	.890	N/A	3447	7600	76.20	1081	N/A	N/A	N/A	N/A	N/A	N/A
99V-18	99	325	.876	7.92	3.12	1.025	.00282	3050	6725	67.25	956	4800	337.55	3.312	6740	473.98	4.651
99V-19	99	325	.879	7.37	2.90	.824	N/A	3504	7725	77.25	1098	N/A	N/A	N/A	N/A	N/A	N/A
99V-21	99	325	.885	8.00	3.15	.845	.00266	4853	10700	107.00	1522	5730	402.95	3.954	6970	490.16	4.809
99V-22	99	325	.883	N/A	N/A	N/A	N/A	3935	8675	86.75	1234	N/A	N/A	N/A	N/A	N/A	N/A
99V-23	99	325	.883	7.90	3.11	1.399	.00420	5375	11850	118.50	1685	4000	281.29	2.760	5450	383.26	3.760
99V-24	99	325	.879	8.18	3.22	.980	N/A	4513	9950	99.50	1415	N/A	N/A	N/A	N/A	N/A	N/A
99V-25	99	325	.883	7.34	2.89	.970	"	4479	9850	98.49	1401	"	"	"	"	"	"
99V-26	99	325	.879	N/A	N/A	N/A	"	3118	6875	68.75	978	"	"	"	"	"	"
99V-27	99	325	.880	7.62	3.00	.884	N/A	4040	8900	89.00	1266	N/A	N/A	N/A	N/A	N/A	N/A

Spec no.	Depth (m)	Depth (ft)	Density (g/cm^3)	Press speed (cm/min)	Press speed (in./min)	Time to failure (sec)	Strain at failure	Load at failure (kg)	Load at failure (lb)	Stress at failure (kg/cm^2)	Stress at failure (psi)	Secant modulus psi $X10^3$	Secant modulus kg/cm^2 $X10^3$	Secant modulus dyn/cm^2 $X10^{10}$	Tangent modulus psi $X10^3$	Tangent modulus kg/cm^2 $X10^3$	Tangent modulus dyn/cm^2 $X10^{10}$
20H-1	20	66	.637	7.21	2.84	.465	.00155	1043	2300	23.00	327	2110	148.38	1.456	3390	238.40	2.339
20H-2	20	66	.630	8.43	3.32	.400	.00162	800	1765	17.65	251	1560	109.71	1.076	2750	193.39	1.898
20H-3	20	66	.648	8.61	3.39	.520	.00259	1397	3080	30.80	438	1690	118.85	1.166	2500	175.81	1.725
20H-4	20	66	.624	10.44	4.11	.440	.00219	1029	2270	22.70	323	1470	103.38	1.104	2220	156.12	1.532
20H-5	20	66	.622	10.16	4.00	.450	.00229	1134	2500	25.00	356	1550	109.00	1.070	2320	163.15	1.601
20H-6	20	66	.612	11.15	4.39	.450	.00200	1043	2300	23.00	327	1680	118.14	1.159	2490	175.10	1.718
20H-7	20	66	.626	7.42	2.92	.395	N/A	952	2100	21.00	299	N/A	N/A	N/A	N/A	N/A	N/A
20H-9	20	66	.635	9.45	3.72	.460	.00146	1197	2640	26.40	375	2570	180.73	1.773	3690	259.49	2.546
20H-10	20	66	.614	9.24	3.64	.415	.00175	986	2175	21.75	309	1770	124.47	1.221	2640	185.65	1.822
20H-12	20	66	.646	11.02	4.34	.465	.00238	1238	2730	27.30	388	1630	114.63	1.125	2350	165.26	1.622
20H-13	20	66	.628	9.75	3.84	.385	.00162	970	2140	21.40	304	1870	131.51	1.290	2510	176.51	1.732
80H-1	80	262	.867	9.22	3.63	.774	N/A	3515	7750	77.70	1105	N/A	N/A	N/A	N/A	N/A	N/A
80H-2	80	262	.851	10.72	4.22	.498	"	2347	5175	51.88	738	"	"	"	"	"	"
80H-3	80	262	.856	10.34	4.07	.612	"	2322	5120	51.33	730	"	"	"	"	"	"
80H-4	80	262	.850	10.26	4.04	.774	"	3300	7275	72.75	1034	"	"	"	"	"	"
80H-5	80	262	.864	11.00	4.33	.702	"	2912	6420	64.20	913	"	"	"	"	"	"
80H-6	80	262	.870	8.48	3.34	.750	"	4513	9950	99.50	1415	"	"	"	"	"	"
80H-9	80	262	.852	9.40	3.70	.738	N/A	4345	9850	98.50	1401	N/A	N/A	N/A	N/A	N/A	N/A
99H-1	99	325	.885	8.56	3.37	1.124	.00379	4540	10020	100.20	1425	3860	271.45	2.663	5470	384.67	3.774
99H-3	99	325	.883	8.26	3.25	1.159	.00340	5205	11475	114.44	1628	4800	337.55	3.312	6170	433.90	4.257
99H-4	99	325	.885	8.53	3.36	1.084	.00322	4967	10950	109.50	1557	4840	340.37	3.340	6350	446.55	4.381
99H-5	99	325	.883	8.86	3.49	.899	.00295	3685	8125	81.03	1157	3910	274.97	2.698	5550	390.30	3.830
99H-6	99	325	.884	8.94	3.52	.884	N/A	5239	11550	115.50	1638	N/A	N/A	N/A	N/A	N/A	N/A
99H-7	99	325	.887	8.69	3.42	1.049	.00319	4729	10425	104.25	1483	4650	327.00	3.208	6350	446.55	4.382
99H-9	99	325	.883	8.36	3.29	.959	.00270	4071	8975	89.75	1276	4740	333.33	3.271	6720	472.57	4.637
99H-10	99	325	.886	8.20	3.23	.886	.00217	3663	8075	80.96	1151	5330	374.82	3.678	7150	502.81	4.934
99H-11	99	325	.879	8.20	3.23	.879	.00238	4071	8975	89.75	1276	5360	377.34	3.698	7150	502.81	4.934

APPENDIX C. CAMP CENTURY RING-TENSILE STRENGTH DATA AT –25C.

Snow samples, 7.6 cm (30 in.) in diameter.

Spec no.	Depth (m)	Depth (ft)	Length (cm)	Length (in.)	Density (g/cm³)	Press speed (cm/min)	Press speed (in./min)	Strain at failure	Load at failure (kg)	Load at failure (lb.)	Stress at failure (kg/cm²)	Stress at failure (psi)
P-1	From surface pit		6.9	1.84	.537	N/A	N/A	N/A	78	172	6.70	95
P-2	"		7.3	2.22	.482	"	"	"	63	139	5.09	72
P-3	"		7.4	2.32	.523	"	"	"	101	223	8.08	115
P-4	"		7.3	2.22	.471	"	"	"	47	104	3.84	55
P-5	"		7.0	1.92	.474	"	"	"	74	163	6.19	88
P-6	"		7.5	2.42	.533	"	"	"	101	223	7.99	114
P-7	"		7.1	2.02	.475	"	"	"	63	139	5.24	74
P-8	"		6.7	1.62	.483	"	"	"	56	123	4.96	71
P-9	"		7.2	2.12	.476	"	"	"	N/A	N/A	N/A	N/A
P-10	"		7.6	2.52	.507	28.2	11.10	.55	60	132	4.68	67
P-11	"		7.7	3.03	.506	36.9	14.53	.53	64	141	4.97	71
P-12	"		7.6	2.99	.513	N/A	N/A	N/A	72	159	5.56	79
P-13	"		7.9	3.11	.518	"	"	"	69	152	5.20	74
P-14	"		6.8	2.67	.485	"	"	"	56	123	4.93	70
P-15	"		6.3	2.48	.500	28.9	11.38	.86	53	117	4.89	69
P-16	"		8.1	3.18	.512	N/A	N/A	N/A	67	148	4.95	70
P-17	"		7.3	2.87	.472	"	"	"	50	110	4.07	58
P-18	"		5.3	2.08	.480	"	"	"	37	82	4.15	59
P-19	"		8.0	3.14	.423	"	"	"	44	97	3.24	46
P-20	"		7.3	2.87	.419	"	"	"	38	84	3.09	44
P-21	"		8.0	3.15	.507	23.6	9.29	.40	73	161	5.46	78
P-22	"		7.7	3.03	.516	N/A	N/A	N/A	82	181	6.34	90
P-23	"		7.1	2.79	.442	"	"	"	37	82	3.12	44
P-24	"		8.9	3.50	.467	"	"	"	58	128	3.88	55
P-25	"		7.5	2.95	.444	28.2	11.10	.52	46	101	3.68	52
P-26	"		6.8	2.67	.436	N/A	N/A	N/A	39	86	3.41	48
P-27	"		6.5	2.56	.506	"	"	"	56	123	5.17	73
P-28	"		8.0	3.15	.501	"	"	"	63	139	4.69	67
P-29	"		7.5	2.95	.550	"	"	"	74	163	5.91	84
P-30	"		6.9	2.72	.482	"	"	"	56	123	4.81	68
P-31	"		7.3	2.87	.520	28.7	11.29	.53	64	141	5.14	73
P-32	"		8.2	3.22	.516	N/A	N/A	N/A	92	203	6.61	94
P-33	From surface pit		6.9	2.72	.483	N/A	N/A	N/A	47	104	4.07	58
P-34	"		6.7	2.64	.518	"	"	"	61	134	5.40	77
P-35	"		8.4	3.31	.503	27.3	10.74	.49	66	145	4.66	66
P-36	"		7.5	2.95	.518	N/A	N/A	N/A	65	143	5.15	73
P-37	"		7.4	2.91	.496	"	"	"	56	123	4.49	64
P-38	"		5.3	2.09	.489	"	"	"	47	104	5.29	75
P-39	"		8.1	3.19	.522	"	"	"	83	183	6.13	87
P-40	"		6.1	2.40	.483	"	"	"	47	104	4.62	66
P-41	"		4.7	1.85	.516	22.9	9.02	.27	48	106	6.04	86
P-42	"		6.8	2.68	.476	N/A	N/A	N/A	50	110	4.36	62
P-43	"		5.8	2.28	.509	"	"	"	47	104	4.81	68
P-44	"		6.6	2.60	.502	"	"	"	58	128	5.23	74
P-45	"		7.2	2.83	.475	27.8	10.94	.97	62	137	5.10	72
P-46	"		6.4	2.52	.484	N/A	N/A	N/A	44	97	4.09	58
P-47	"		8.0	3.14	.482	"	"	"	60	132	4.43	63
P-48	"		7.1	2.79	.418	27.8	12.20	.62	34	75	2.82	40
P-49	"		6.1	2.40	.508	N/A	N/A	N/A	50	110	4.83	69
P-50	"		8.7	3.42	.508	"	"	"	50	110	4.83	69
P-51	"		7.7	3.03	.527	27.3	10.79	.35	85	187	6.58	93
P-52	"		7.3	2.87	.495	N/A	N/A	N/A	56	123	4.56	65
P-53	"		7.8	3.07	.482	"	"	"	55	121	4.23	60
P-54	"		6.4	2.52	.534	"	"	"	73	161	6.71	95
P-55	"		7.2	2.83	.550	24.6	9.68	.29	79	174	6.48	92
P-56	"		6.5	2.56	.418	N/A	N/A	N/A	30	66	2.74	39
P-57	"		7.2	2.83	.486	"	"	"	53	117	4.31	61
P-58	"		7.2	2.83	.426	"	"	"	34	75	2.85	40
P-59	"		6.7	2.64	.506	27.1	10.67	.43	62	137	5.50	78
P-60	"		7.7	3.03	.552	N/A	N/A	N/A	82	181	6.31	90
P-61	"		6.7	2.64	.474	"	"	"	47	104	4.17	59
P-62	"		7.4	2.91	.470	"	"	"	46	101	3.69	52
P-63	"		7.4	2.91	.503	"	"	"	64	141	5.11	73
P-64	"		8.1	3.19	.510	"	"	"	81	179	5.92	84
P-65	"		7.7	3.03	.505	25.7	10.12	.66	72	159	5.54	79

Spec. no.	Depth (m)	Depth (ft)	Length (cm)	Length (in.)	Density (g/cm³)	Press speed (cm/min)	Press speed (in./min)	Strain at failure	Load at failure (kg)	Load at failure (lb.)	Stress at failure (kg/cm²)	Stress at failure (psi)
20V-1	20	66	7.6	2.99	.612	22.2	8.74	.25	111	245	8.67	123
20V-2	20	66	7.8	3.07	.610	N/A	N/A	N/A	102	225	7.83	111
20V-3	20	66	8.3	3.27	.588	"	"	"	120	265	8.57	122
20V-4	20	66	6.5	2.56	N/A	"	"	"	N/A	N/A	N/A	N/A
20V-5	20	66	7.6	2.99	.599	"	"	"	101	223	7.84	111
20V-6	20	66	7.1	2.80	.612	22.4	8.82	.23	95	209	7.94	113
20V-7	20	66	8.2	3.23	.606	N/A	N/A	N/A	125	276	9.05	129
20V-8	20	66	7.6	2.99	.606	"	"	"	109	240	8.53	121
20V-9	20	66	7.3	2.87	.619	20.6		.19	113	249	9.19	131
20V-10	20	66	6.9	2.72	.585	N/A	N/A	N/A	109	240	9.33	133
20V-11	20	66	6.6	2.60	.578	"	"	"	75	165	6.73	96
20V-12	20	66	7.9	3.11	.586	"	"	"	108	238	8.09	115
20V-13	20	66	8.0	3.15	.617	19.9	8.11	.46	104	229	7.78	111
20V-14	20	66	7.3	2.87	.597	N/A	N/A	N/A	83	183	6.71	95
20V-15	20	66	7.7	3.03	.591	"	"	"	109	240	8.38	119
20V-16	20	66	7.6	2.99	.590	"	"	"	92	203	7.18	102
20V-17	20	66	5.7	2.24	.584	"	"	"	71	156	7.41	105
20V-18	20	66	7.3	2.87	.592	"	"	"	92	203	7.49	106
20V-19	20	66	5.4	2.12	.602	11.8	4.64	.38	91	201	9.92	141
20V-20	20	66	7.5	2.95	.604	N/A	N/A	N/A	102	225	8.07	115
20V-21	20	66	5.5	2.16	.588	20.5	8.07	.60	74	163	7.91	112
20V-22	20	66	7.5	2.95	.585	N/A	N/A	N/A	103	227	8.18	116
20V-23	20	66	7.6	2.99	.612	10.4	4.09	.34	116	256	9.06	129
20V-24	20	66	8.3	3.27	.617	N/A	N/A	N/A	137	302	9.85	140
20V-25	20	66	8.3	3.27	.618	"	"	"	126	278	9.05	129
20V-26	20	66	6.8	2.67	.593	"	"	"	90	198	7.86	112
20V-27	20	66	6.6	2.60	.597	"	"	"	84	185	7.64	109
20V-28	20	66	7.1	2.79	.593	22.7	8.93	.56	107	236	8.96	127
20V-29	20	66	6.5	2.56	.586	N/A	N/S	N/A	101	223	9.23	131
20V-30	20	66	7.2	2.82	.614	22.3	8.78	.48	111	245	9.13	130
20V-31	20	66	6.4	2.52	.590	N/A	N/A	N/A	102	225	9.37	133
20V-32	20	66	7.5	2.95	.586	"	"	"	101	223	8.02	114
20V-33	20	66	7.3	2.87	.625	21.2	8.35	.38	121	267	9.82	140
20V-34	20	66	6.9	2.72	.589	N/A	N/A	N/A	95	209	8.18	116
20V-35	20	66	7.1	2.77	.590	"	"	"	100	220	8.41	119
20V-36	20	66	5.9	2.31	.608	"	"	"	91	200	9.18	130
20V-37	20	66	6.6	2.59	.608	22.7	8.93	.42	101	223	9.06	129
20V-38	20	66	7.1	2.78	.588	N/A	N/A	N/A	102	225	8.52	121
20V-39	20	66	6.7	2.64	.585	"	"	"	64	141	5.68	81
20V-40	20	66	8.1	3.18	.583	21.3	8.38	.48	109	240	7.98	113
30V-1	30	98	8.1	3.18	.662	19.1	7.52	.52	158	348	11.59	165
30V-2	30	98	7.4	2.92	.659	N/A	N/A	N/A	108	238	8.63	123
30V-3	30	98	8.0	3.16	.668	"	"	"	125	276	9.26	132
30V-4	30	98	8.0	3.16	.661	18.3	7.20	.46	161	355	11.93	170
30V-5	30	98	6.8	2.67	.658	N/A	N/A	N/A	120	265	10.48	149
30V-6	30	98	7.5	2.94	.666	"	"	"	154	339	12.23	174
30V-7	30	98	7.2	2.80	.659	"	"	"	128	282	10.63	151
30V-8	30	98	8.4	3.31	.664	"	"	"	132	291	9.27	132
30V-9	30	98	7.7	3.04	.666	"	"	"	163	359	12.53	178
30V-10	30	98	8.5	3.34	.661	"	"	"	203	448	14.18	202
30V-11	30	98	6.3	2.47	.669	"	"	"	124	273	11.74	167
30V-12	30	98	7.5	2.95	.672	17.6	6.93	.38	126	278	9.97	142
30V-13	30	98	7.9	3.09	.655	N/A	N/A	N/A	134	295	10.13	144
30V-14	30	98	7.6	2.97	.673	24.8	9.76	.56	136	300	10.68	152
30V-15	30	98	8.2	3.23	.669	19.5	7.68	.56	198	436	14.31	203
37V-1	37	121	8.3	3.25	.727	15.8	6.22	.30	188	414	13.50	192
37V-2	37	121	8.0	3.14	.698	N/A	N/A	N/A	132	291	9.77	139
37V-3	37	121	7.6	3.00	.685	23.4	9.21	.42	125	276	9.70	138
37V-4	37	121	6.5	2.55	.685	N/A	N/A	N/A	127	280	11.64	165
37V-5	37	121	7.7	3.04	.709	18.6	7.32	.40	177	390	13.59	193
37V-6	37	121	7.1	2.78	.700	N/A	N/A	N/A	116	256	9.70	138
37V-7	37	121	8.2	3.22	.706	"	"	"	154	339	11.18	159
37V-8	37	121	7.7	3.01	.694	20.8	8.19	.48	147	324	11.43	162
37V-9	37	121	7.2	2.81	.689	N/A	N/A	N/A	118	260	9.80	139
50V-1	50	164	6.9	2.72	.724	17.9	7.05	.84	154	339	13.28	189
50V-2	50	164	7.7	3.04	.731	N/A	N/A	N/A	168	370	12.90	183

Spec no.	Depth (m)	Depth (ft)	Length (cm)	Length (in.)	Density (g/cm³)	Press speed (cm/min)	Press speed (in./min)	Strain at failure	Load at failure (kg)	Load at failure (lb.)	Stress at failure (kg/cm²)	Stress at failure (psi)
50V-3	50	164	8.2	3.21	.739	N/A	N/A	N/A	116	256	8.40	119
50V-4	50	164	7.2	2.82	.738	20.1	7.91	1.02	179	395	14.80	210
50V-5	50	164	7.1	2.78	.741	N/A	N/A	N/A	138	304	11.61	165
50V-6	50	164	8.0	3.16	.736	"	"	"	136	300	10.24	146
50V-7	50	164	8.1	3.16	.731	21.0	8.27	.78	156	344	11.55	164
50V-8	50	164	7.8	3.10	.743	N/A	N/A	N/A	163	359	12.39	176
50V-9	50	164	6.7	2.64	.768	"	"	"	113	249	10.01	142
50V-10	50	164	7.3	2.87	.770	17.5	6.89	1.06	229	505	18.64	265
50V-11	50	164	7.0	2.74	.741	N/A	N/A	N/A	127	280	10.81	154
50V-12	50	164	7.7	3.02	.752	"	"	"	177	390	13.68	194
50V-13	50	164	7.1	2.80	.772	"	"	"	186	410	15.49	220
50V-14	50	164	7.7	3.02	.730	20.2	7.95	.80	147	324	11.40	162
57V-1	57	187	7.1	2.80	.808	19.5	7.68	1.28	231	509	19.24	274
57V-2	57	187	7.6	2.98	.801	N/A	N/A	N/A	193	425	15.11	215
57V-3	57	187	7.4	2.91	.754	"	"	"	186	410	14.93	212
57V-4	57	187	8.1	3.19	.786	16.6	6.53	.84	220	485	16.09	229
57V-5	57	187	6.6	2.58	.800	N/A	N/A	N/A	181	399	16.38	233
57V-6	57	187	8.3	3.19	.802	"	"	"	244	538	17.51	249
57V-7	57	187	8.1	3.19	.774	"	"	"	177	390	12.96	184
57V-8	57	187	8.0	3.14	.767	18.7	7.36	1.16	200	441	14.82	211
57V-9	57	187	6.9	2.72	.776	N/A	N/A	N/A	138	304	11.86	169
57V-10	57	187	7.7	3.03	.806	"	"	"	245	540	18.87	268
57V-11	57	187	7.9	3.10	.800	16.9	6.65	.86	227	500	17.10	243
72V-1	72	236	7.1	2.79	.833	18.1	7.12	1.12	272	600	22.74	323
72V-2	72	236	7.1	2.79	.828	N/A	N/A	N/A	172	379	14.40	205
72V-3	72	236	6.6	2.61	.837	"	"	"	258	569	23.13	329
72V-4	72	236	5.8	2.27	.798	"	"	"	147	324	15.15	215
72V-5	72	236	7.2	2.83	.846	"	"	"	244	538	20.18	287
72V-6	72	236	8.2	3.21	.831	"	"	"	227	500	16.47	234
72V-7	72	236	7.3	2.87	.821	16.6	6.53	.84	227	500	18.45	262
72V-8	72	236	6.3	2.47	.838	N/A	N/A	N/A	290	639	27.46	390
72V-9	72	236	7.0	2.75	.812	"	"	"	408	900	34.64	493
72V-10	72	236	7.8	3.07	.821	16.1	6.34	.80	229	505	17.40	247
72V-11	72	236	7.6	2.99	.816	N/A	N/A	N/A	218	481	16.99	241
72V-12	72	236	8.3	3.25	.818	16.1	6.34	.80	258	569	18.55	264
72V-13	72	236	7.3	2.88	.621	N/A	N/A	N/A	415	915	33.63	478
80V-1	80	262	8.5	3.34	N/A	"	"	"	N/A	N/A	N/A	N/A
80V-2	80	262	6.1	2.40	.847	17.9	7.05	.84	177	390	17.23	245
80V-3	80	262	7.8	3.08	.839	N/A	N/A	N/A	408	900	30.97	440
80V-4	80	262	7.2	2.84	.844	"	"	"	213	470	17.49	249
80V-5	80	262	7.9	3.10	.860	"	"	"	422	930	31.80	452
80V-6	80	262	7.1	2.81	.846	19.4	7.64	.94	184	406	15.28	217
80V-7	80	262	6.5	2.56	.834	N/A	N/A	N/A	186	410	16.97	241
80V-8	80	262	6.8	2.66	.843	"	"	"	195	430	17.14	244
80V-9	80	262	7.3	2.86	.861	16.6	6.53	.84	238	525	19.46	277
80V-10	80	262	7.9	3.11	.832	N/A	N/A	N/A	413	911	30.96	440
80V-11	80	262	5.8	2.26	.860	"	"	"	141	311	14.50	206
80V-12	80	262	7.8	3.08	.852	"	"	"	218	481	16.50	235
80V-13	80	262	6.4	2.49	.830	"	"	"	150	331	14.00	199
80V-14	80	262	6.8	2.69	.863	14.5	5.71	.54	166	366	14.38	204
80V-15	80	262	7.2	2.83	.857	N/A	N/A	N/A	209	461	17.19	244
80V-16	80	262	6.4	2.49	.855	"	"	"	134	295	12.52	178
80V-17	80	262	5.3	2.08	.863	"	"	"	109	240	12.22	174
80V-18	80	262	8.6	3.38	.851	17.9	7.05	1.00	231	509	15.98	227
85V-1	85	279	8.4	3.29	.850	N/A	N/A	N/A	293	646	20.74	295
85V-2	85	279	8.4	3.32	.862	16.5	6.48	.94	254	560	17.88	254
85V-3	85	279	6.4	2.50	.868	N/A	N/A	N/A	227	500	21.15	301
85V-4	85	279	7.8	3.04	.860	16.1	6.32	.84	227	500	17.38	247
85V-5	85	279	7.4	2.91	.866	N/A	N/A	N/A	270	595	21.66	308
85V-6	85	279	7.5	2.93	.868	"	"	"	186	410	14.81	210
85V-7	85	279	7.9	3.10	.867	16.1	6.32	.80	261	575	19.64	279
85V-8	85	279	7.5	2.95	.865	N/A	N/A	N/A	193	425	15.25	217
85V-9	85	279	9.0	3.54	.870	"	"	"	222	489	14.64	208
85V-10	85	279	8.6	3.37	.866	"	"	"	290	639	20.10	286
85V-11	85	279	8.4	3.32	.852	15.0	5.89	1.06	352	776	24.71	351

Spec no.	Depth (m)	Depth (ft)	Length (cm)	Length (in.)	Density (g/cm³)	Press speed (cm/min)	Press speed (in./min)	Strain at failure	Load at failure (kg)	Load at failure (lb.)	Stress at failure (kg/cm²)	Stress at failure (psi)
99V-1	99	325	8.4	3.31	.879	N/A	N/A	N/A	447	986	31.48	448
99V-2	99	325	8.5	3.36	.874	16.1	6.32	.98	345	761	23.98	341
99V-3	99	325	7.6	2.98	.880	N/A	N/A	N/A	206	454	16.16	230
99V-4	99	325	7.5	2.95	.876	"	"	"	336	741	26.55	378
99V-5	99	325	7.8	3.08	.874	"	"	"	358	789	27.18	386
99V-6	99	325	8.0	3.14	.884	"	"	"	335	739	24.92	354
99V-7	99	325	8.2	3.21	.867	"	"	"	315	694	22.92	326
99V-8	99	325	6.4	2.50	.879	16.1	6.32	.84	254	560	23.69	337
99V-10	99	325	7.3	2.86	.885	N/A	N/A	N/A	349	769	28.50	405
99V-11	99	325	8.0	3.14	.875	16.1	6.32	.96	324	714	24.11	343
99V-12	99	325	8.5	3.34	.885	16.1	6.32	1.40	463	1021	32.33	460
99V-13	99	325	7.7	3.02	.877	N/A	N/A	N/A	306	675	23.68	337
99V-14	99	325	7.4	2.93	.885	"	"	"	338	745	26.94	383
99V-15	99	325	7.3	2.86	.887	"	"	"	297	655	24.27	345
20H-1	20	66	7.8	3.07	.616	22.6	8.90	.58	124	273	9.45	134
20H-2	20	66	6.4	2.51	.625	N/A	N/A	N/A	90	198	8.35	119
20H-3	20	66	6.9	2.71	.619	"	"	"	90	198	7.73	110
20H-4	20	66	6.6	2.61	.622	"	"	"	94	207	8.44	120
20H-5	20	66	6.5	2.56	.610	"	"	"	92	203	8.36	119
20H-6	20	66	7.6	2.99	.619	"	"	"	109	240	8.51	121
20H-7	20	66	6.8	2.66	.627	"	"	"	127	280	11.14	158
20H-8	20	66	7.2	2.81	.634	21.4	8.42	.54	122	269	10.16	144
20H-9	20	66	7.6	2.97	.631	N/A	N/A	N/A	118	260	9.25	131
20H-10	20	66	8.0	3.14	.618	"	"	"	128	282	9.51	135
20H-11	20	66	7.2	2.83	.627	22.7	8.94	.44	102	225	8.37	117
20H-12	20	66	6.4	2.50	.630	N/A	N/A	N/A	88	194	8.21	117
20H-13	20	66	7.3	2.88	.629	"	"	"	112	247	9.13	130
20H-14	20	66	7.7	3.03	.621	20.3	8.00	.48	119	262	9.16	130
20H-15	20	66	7.7	3.03	.630	N/A	N/A	N/A	105	231	8.11	115
80H-1	80	262	7.9	3.10	.848	14.2	5.59	.56	227	500	17.10	243
80H-2	80	262	8.3	3.27	.847	N/A	N/A	N/A	347	765	26.72	380
80H-3	80	262	5.5	2.15	.841	"	"	"	170	375	18.47	263
80H-4	80	262	7.6	2.97	.846	"	"	"	340	750	26.73	380
80H-5	80	262	6.4	2.53	.842	16.1	6.34	.76	229	505	21.13	300
80H-6	80	262	7.8	3.05	.862	N/A	N/A	N/A	306	675	23.38	332
80H-7	80	262	7.4	2.89	.865	"	"	"	158	348	12.83	182
80H-8	80	262	8.8	3.45	.862	"	"	"	313	690	21.20	301
80H-9	80	262	8.1	3.17	.863	15.1	5.94	.84	267	589	19.72	280
80H-10	80	262	7.8	3.04	.854	N/A	N/A	N/A	222	489	17.04	242
80H-11	80	262	7.4	2.90	.851	"	"	"	141	311	11.32	161
80H-12	80	262	7.8	3.05	.871	17.0	6.69	.84	226	498	17.36	247
80H-13	80	262	8.5	3.34	.854	N/A	N/A	N/A	328	723	22.95	326
80H-14	80	262	8.2	3.23	.864	"	"	"	283	624	20.44	291
80H-15	80	262	6.6	2.60	.847	"	"	"	222	489	19.94	283
80H-16	80	262	7.2	2.82	.866	16.1	6.34	.84	315	694	26.08	371
99H-1	99	325	6.9	2.72	.874	16.1	6.34	1.16	274	604	23.56	335
99H-2	99	325	8.0	3.15	.880	16.1	6.34	.90	299	659	22.14	315
99H-3	99	325	8.9	3.48	.882	10.8	4.25	.80	431	950	28.89	411
99H-4	99	325	7.0	2.76	.882	N/A	N/A	N/A	352	776	29.70	422
99H-5	99	325	8.0	3.16	.875	16.1	6.34	.80	229	505	16.92	241
99H-6	99	325	7.4	2.89	.878	16.1	6.34	.50	138	304	11.18	159
99H-7	99	325	7.9	3.10	.878	N/A	N/A	N/A	274	604	20.63	293
99H-8	99	325	7.4	2.89	.880	12.4	4.88	1.00	399	880	32.21	458
99H-10	99	325	8.0	3.14	.880	11.5	4.53	.60	281	620	20.88	297
99H-11	99	325	5.9	2.33	.879	19.4	7.64	1.20	159	350	15.88	226
99H-12	99	325	7.6	3.00	.862	14.2	5.59	.70	200	441	15.54	221
99H-13	99	325	8.1	3.18	.873	12.5	4.92	.70	318	701	23.28	331
99H-14	99	325	7.5	2.96	.878	13.1	5.16	.70	272	600	21.47	305
99H-15	99	325	6.4	2.51	.873	15.3	6.02	.72	181	399	16.89	240

APPENDIX D. UNCONFINED COMPRESSIVE STRENGTH OF CAMP CENTURY VERTICAL SNOW SAMPLES 8.25 IN. LENGTH, 3.0 IN. DIAM AT –25C.

Values computed from eq 1.

DEPTH (FT)	DEPTH (M)	DENSITY (GM/CM3)	STRENGTH (PSI)	STRENGTH (KG/CM2)	POROSITY (N)	DEPTH (FT)	DEPTH (M)	DENSITY (GM/CM3)	STRENGTH (PSI)	STRENGTH (KG/CM2)	POROSITY (N)
*	*	.350	36	2.57	.620	10	3.3	.422	74	5.18	.541
*	*	.352	37	2.59	.617	11	3.4	.424	75	5.30	.539
*	*	.354	37	2.61	.615	11	3.5	.426	77	5.41	.537
*	*	.356	38	2.64	.613	11	3.6	.428	79	5.53	.535
*	*	.358	38	2.67	.611	12	3.7	.430	80	5.65	.533
*	*	.360	39	2.71	.609	12	3.8	.432	82	5.77	.530
*	*	.362	39	2.75	.607	12	4.0	.434	84	5.90	.528
*	*	.364	40	2.79	.604	13	4.1	.436	86	6.02	.526
*	*	.366	40	2.84	.602	13	4.2	.438	87	6.15	.524
*	*	.368	41	2.89	.600	14	4.3	.440	89	6.27	.522
*	*	.370	42	2.94	.598	14	4.4	.442	91	6.40	.520
3	1.0	.372	43	2.99	.596	14	4.5	.444	93	6.53	.517
3	1.1	.374	43	3.05	.593	15	4.6	.446	95	6.67	.515
3	1.1	.376	44	3.11	.591	15	4.7	.448	97	6.80	.513
3	1.2	.378	45	3.17	.589	15	4.9	.450	99	6.93	.511
4	1.3	.380	46	3.24	.587	16	5.0	.452	101	7.07	.509
4	1.3	.382	47	3.31	.585	16	5.1	.454	102	7.20	.507
4	1.4	.384	48	3.38	.583	17	5.2	.456	104	7.34	.504
4	1.5	.386	49	3.45	.580	17	5.3	.458	106	7.48	.502
5	1.6	.388	50	3.53	.578	17	5.4	.460	108	7.62	.500
5	1.7	.390	51	3.61	.576	18	5.5	.462	110	7.76	.498
5	1.8	.392	53	3.69	.574	18	5.6	.464	112	7.91	.496
6	1.9	.394	54	3.78	.572	18	5.8	.466	114	8.05	.493
6	1.9	.396	55	3.86	.570	19	5.9	.468	117	8.19	.491
6	2.0	.398	56	3.95	.567	19	6.0	.470	119	8.34	.489
7	2.1	.400	58	4.04	.565	20	6.1	.472	121	8.49	.487
7	2.2	.402	59	4.14	.563	20	6.2	.474	123	8.63	.485
7	2.3	.404	60	4.23	.561	20	6.3	.476	125	8.78	.483
8	2.4	.406	62	4.33	.559	21	6.5	.478	127	8.93	.480
8	2.5	.408	63	4.43	.557	21	6.6	.480	129	9.08	.478
8	2.7	.410	64	4.53	.554	21	6.7	.482	131	9.23	.476
9	2.8	.412	66	4.64	.552	22	6.8	.484	133	9.39	.474
9	2.9	.414	67	4.74	.550	22	6.9	.486	136	9.54	.472
9	3.0	.416	69	4.85	.548	23	7.1	.488	138	9.69	.470
10	3.1	.418	71	4.96	.546	23	7.2	.490	140	9.85	.467
10	3.2	.420	72	5.07	.543	24	7.3	.492	142	10.00	.465
24	7.4	.494	144	10.16	.463	44	13.5	.566	232	16.33	.385
24	7.6	.496	147	10.32	.461	45	13.7	.568	235	16.52	.383
25	7.7	.498	149	10.48	.459	45	14.0	.570	238	16.70	.380
25	7.8	.500	151	10.64	.457	46	14.2	.572	240	16.89	.378
26	8.0	.502	154	10.80	.454	47	14.4	.574	243	17.08	.376
26	8.1	.504	156	10.96	.452	48	14.7	.576	246	17.27	.374
27	8.2	.506	158	11.12	.450	48	14.9	.578	248	17.47	.372
27	8.4	.508	160	11.28	.448	49	15.2	.580	251	17.66	.370
27	8.5	.510	163	11.44	.446	50	15.4	.582	254	17.85	.367
28	8.7	.512	165	11.61	.443	51	15.7	.584	257	18.05	.365
28	8.8	.514	167	11.77	.441	52	15.9	.586	259	18.24	.363
29	9.0	.516	170	11.94	.439	53	16.2	.588	262	18.44	.361
29	9.1	.518	172	12.10	.437	53	16.5	.590	265	18.64	.359
30	9.3	.520	175	12.27	.435	54	16.7	.592	268	18.84	.356
30	9.4	.522	177	12.44	.433	55	17.0	.594	271	19.04	.354
31	9.6	.524	179	12.61	.430	56	17.3	.596	274	19.24	.352
31	9.7	.526	182	12.78	.428	57	17.6	.598	277	19.45	.350
32	9.9	.528	184	12.95	.426	58	17.9	.600	279	19.65	.348
32	10.0	.530	187	13.12	.424	59	18.1	.602	282	19.86	.346
33	10.2	.532	189	13.29	.422	60	18.4	.604	285	20.06	.343
34	10.4	.534	191	13.46	.420	61	18.7	.606	288	20.27	.341
34	10.5	.536	194	13.64	.417	62	19.0	.608	291	20.48	.339
35	10.7	.538	196	13.81	.415	63	19.4	.610	294	20.70	.337
35	10.9	.540	199	13.98	.413	64	19.7	.612	297	20.91	.335
36	11.1	.542	201	14.16	.411	65	20.0	.614	300	21.12	.333
36	11.3	.544	204	14.34	.409	66	20.3	.616	303	21.34	.330
37	11.5	.546	206	14.51	.406	67	20.6	.618	307	21.56	.328
38	11.6	.548	209	14.69	.404	68	21.0	.620	310	21.78	.326
38	11.8	.550	211	14.87	.402	69	21.3	.622	313	22.00	.324
39	12.0	.552	214	15.05	.400	70	21.6	.624	316	22.22	.322
40	12.2	.554	217	15.23	.398	72	22.0	.626	319	22.45	.320
40	12.4	.556	219	15.41	.396	73	22.3	.628	322	22.68	.317
41	12.6	.558	222	15.59	.393	74	22.7	.630	326	22.91	.315
42	12.9	.560	224	15.78	.391	75	23.0	.632	329	23.14	.313
42	13.1	.562	227	15.96	.389	76	23.4	.634	332	23.37	.311
43	13.3	.564	230	16.44	.387	77	23.7	.636	336	23.60	.309

DEPTH (FT)	DEPTH (M)	DENSITY (GM/CM3)	STRENGTH (PSI)	STRENGTH (KG/CM2)	POROSITY (N)
78	24.1	.638	339	23.84	.306
80	24.4	.640	342	24.08	.304
81	24.8	.642	346	24.32	.302
82	25.2	.644	349	24.56	.300
83	25.6	.646	353	24.81	.298
85	25.9	.648	356	25.06	.296
86	26.3	.650	360	25.31	.293
87	26.7	.652	363	25.56	.291
88	27.1	.654	367	25.81	.289
90	27.5	.656	371	26.07	.287
91	27.9	.658	374	26.33	.285
92	28.3	.660	378	26.59	.283
94	28.7	.662	382	26.86	.280
95	29.1	.664	386	27.13	.278
96	29.5	.666	390	27.40	.276
98	29.9	.668	393	27.67	.274
99	30.3	.670	397	27.95	.272
100	30.7	.672	401	28.22	.270
102	31.2	.674	405	28.51	.267
103	31.6	.676	409	28.79	.265
104	32.0	.678	414	29.08	.263
106	32.4	.680	418	29.37	.261
107	32.9	.682	422	29.67	.259
109	33.3	.684	426	29.96	.256
110	33.7	.686	430	30.26	.254
112	34.2	.688	435	30.57	.252
113	34.6	.690	439	30.88	.250
114	35.0	.692	444	31.19	.248
116	35.5	.694	448	31.50	.246
117	35.9	.696	453	31.82	.243
119	36.4	.698	457	32.15	.241
120	36.8	.700	462	32.47	.239
122	37.3	.702	466	32.80	.237
123	37.7	.704	471	33.14	.235
125	38.2	.706	476	33.48	.233
126	38.7	.708	481	33.82	.230
186	56.9	.782	712	50.10	.150
188	57.4	.784	720	50.65	.148
190	58.0	.786	728	51.22	.146
191	58.5	.788	737	51.80	.143
193	59.1	.790	745	52.38	.141
195	59.6	.792	753	52.97	.139
197	60.2	.794	762	53.57	.137
199	60.8	.796	770	54.17	.135
201	61.3	.798	779	54.79	.133
203	61.9	.800	788	55.41	.130
204	62.5	.802	797	56.04	.128
206	63.1	.804	806	56.68	.126
208	63.7	.806	815	57.33	.124
210	64.3	.808	825	57.98	.122
212	64.9	.810	834	58.65	.120
214	65.5	.812	844	59.32	.117
216	66.1	.814	853	60.00	.115
218	66.7	.816	863	60.70	.113
221	67.4	.818	873	61.40	.111
223	68.0	.820	883	62.11	.109
225	68.7	.822	893	62.83	.106
227	69.4	.824	904	63.56	.104
229	70.0	.826	914	64.30	.102
231	70.7	.828	925	65.05	.100
234	71.4	.830	936	65.81	.098
236	72.1	.832	947	66.58	.096
238	72.8	.834	958	67.36	.093
241	73.6	.836	969	68.15	.091
243	74.3	.838	980	68.95	.089
246	75.1	.840	992	69.76	.087
248	75.9	.842	1004	70.59	.085
251	76.7	.844	1016	71.42	.083
254	77.5	.846	1028	72.26	.080
256	78.3	.848	1040	73.12	.078
258	78.7	.850	1052	73.98	.076
262	80.0	.852	1065	74.86	.074
265	80.9	.854	1077	75.75	.072
268	81.8	.856	1090	76.65	.070
271	82.7	.858	1103	77.56	.067
274	83.6	.860	1116	78.49	.065
277	84.6	.862	1129	79.43	.063
280	85.5	.864	1143	80.37	.061
283	86.5	.866	1157	81.33	.059
287	87.6	.868	1170	82.31	.056
290	88.6	.870	1184	83.29	.054
294	89.7	.872	1199	84.29	.052
297	90.8	.874	1213	85.30	.050
301	91.9	.876	1228	86.33	.048
305	93.1	.878	1242	87.37	.046
309	94.3	.880	1257	88.42	.043
313	95.5	.882	1272	89.48	.041
317	96.7	.884	1288	90.56	.039
321	98.0	.886	1303	91.65	.037
325	99.3	.888	1319	92.75	.035
333	101.7	.890	1335	93.87	.033
346	105.6	.892	1351	95.01	.030
361	110.1	.894	1367	96.15	.028
378	115.5	.896	1384	97.31	.026
398	121.6	.898	1401	98.49	.024
421	128.5	.900	1417	99.68	.022
447	136.4	.902	1435	100.89	.020
476	145.2	.904	1452	102.11	.017
508	155.1	.906	1470	103.34	.015
544	166.1	.908	1487	104.59	.013
584	178.3	.910	1505	105.86	.011
628	191.7	.912	1524	107.14	.009
677	206.5	.914	1542	108.44	.006
730	222.6	.916	1561	109.76	.004

THE EXTRAPOLATED -25C STRENGTH OF PURE, (0.920 G/CM2), BUBBLE-FREE ICE IS 1600 PSI OR 112.52 KG/CM2.

* = LESS THAN ONE METER IN DEPTH.

To determine the depth at which a certain density snow is situated, depth-density determinations taken to approximately 99 m in the Inclined Drift at Camp Century (Mock, 1966 unpublished data) were analyzed giving, the following empirical equation:

$$\gamma = 0.341 + 2.9 \times 10^{-2}D - 1.3 \times 10^{-3}D^2 + 3.5 \times 10^{-5}D^3 - 5.0 \times 10^{-7}D^4$$

$$+ 3.6 \times 10^{-9}D^5 - 1.0 \times 10^{-11}D^6$$

where γ and D are given g/cm^3 and m respectively. At depths between 100 and 300 m, the depth-density profile was based on measurements from Site 2 (Langway, 1967), giving:

$$\gamma = 0.909 - 7.1 \times 10^{-3}D + 1.7 \times 10^{-4}D^2 - 1.6 \times 10^{-6}D^3 + 7.7 \times 10^{-9}D^4$$

$$- 1.8 \times 10^{-11}D^5 + 1.64 \times 10^{-14}D^6.$$

DOCUMENT CONTROL DATA - R & D

(Security classification of title, body of abstract and indexing annotation must be entered when the overall report is classified)

1. ORIGINATING ACTIVITY *(Corporate author)*
U.S. Army Cold Regions Research and Engineering Laboratory
Hanover, New Hampshire 03755

2a. REPORT SECURITY CLASSIFICATION
Unclassified

2b. GROUP

3. REPORT TITLE

VARIATION OF SOME MECHANICAL PROPERTIES OF POLAR SNOW, CAMP CENTURY, GREENLAND

4. DESCRIPTIVE NOTES *(Type of report and inclusive dates)*

5. AUTHOR(S) *(First name, middle initial, last name)*
Austin Kovacs, W. F. Weeks and Frank Michitti

6. REPORT DATE
December 1969

7a. TOTAL NO. OF PAGES
34

7b. NO. OF REFS
20

8a. CONTRACT OR GRANT NO.

b. PROJECT NO.

c. DA Task 1T062112A13001 and
DA Task 1T061102B52A02

d.

9a. ORIGINATOR'S REPORT NUMBER(S)
Research Report 276

9b. OTHER REPORT NO(S) *(Any other numbers that may be assigned this report)*

10. DISTRIBUTION STATEMENT
This document has been approved for public release and sale; its distribution is unlimited.

11. SUPPLEMENTARY NOTES

12. SPONSORING MILITARY ACTIVITY
U.S. Army Cold Regions Research and Engineering Laboratory
Hanover, New Hampshire 03755

13. ABSTRACT
The unconfined compressive strengths σ_c and the ring-tensile strengths σ_T of snow and ice specimens from the Inclined Drift at Camp Century, Greenland, were determined. The specimen densities varied over essentially the complete natural density range of polar snow and ice (0.340 to 0.890 g/cm^3). The specimens were loaded rapidly to failure with times varying between 0.2 and 1.4 sec. During loading, head speeds varied between 5.1 and 23.6 cm/min, although during individual tests they were constant. Even the low density specimens failed in the brittle mode. Although a plot of σ_T vs γ is linear, σ_c vs γ is clearly nonlinear. This nonlinearity may result from either changes in the level of the internal stress concentrations associated with the voids in the snow or from changes in the ratio (bulk porosity/effective porosity of the failure surface) with density. Both tangent and secant moduli are linear functions of γ. There is no pronounced change in σ_c with changes in strain rate. A significant increase in σ_T, σ_c and the modulus values was noted at bulk densities greater than 0.830 g/cm^3. This increase is presumably caused by the close-off of the air passages.

14. Key Words

Snow density
Snow mechanical properties
Snow strength tests

DD FORM 1 NOV 65 1473 REPLACES DD FORM 1473, 1 JAN 64, WHICH IS OBSOLETE FOR ARMY USE.